THE ANTENNA LABORATORY

RESEARCH ACTIVITIES in ---

Automatic Controls — *Antennas* — *Echo Area Studies*
Microwave Circuits — *Astronautics* — *E M Field Theory*
Terrain Investigations — *Radomes* — *Systems Analysis*
Wave Propagation — *Submillimeter Applications*

FINAL REPORT
7 September 1962 to 6 September 1963

Study Program Related to Shipboard
Antenna System Environment

Contract N123(953)-31663A

1522-6 6 September 1963

Prepared for:
U.S. Navy Purchasing Office
Los Angeles 55, California

Department of ELECTRICAL ENGINEERING

THE OHIO STATE UNIVERSITY
RESEARCH FOUNDATION
Columbus, Ohio

NOTICES

When Government drawings, specifications, or other data are used for any purpose other than in connection with a definitely related Government procurement operation, the United States Government thereby incurs no responsibility nor any obligation whatsoever, and the fact that the Government may have formulated, furnished, or in any way supplied the said drawings, specifications, or other data, is not to be regarded by implication or otherwise as in any manner licensing the holder or any other person or corporation, or conveying any rights or permission to manufacture, use, or sell any patented invention that may in any way be related thereto.

The Government has the right to reproduce, use, and distribute this report for governmental purposes in accordance with the contract under which the report was produced. To protect the proprietary interests of the contractor and to avoid jeopardy of its obligations to the Government, the report may not be released for non-governmental use such as might constitute general publication without the express prior consent of The Ohio State University Research Foundation.

Qualified requesters may obtain copies of this report from the Defense Documentation Center, Cameron Station, Alexandria, Virginia. Department of Defense contractors must be established for DDC services, or have their "need-to-know" certified by the cognizant military agency of their project or contract.

REPORT

by

THE OHIO STATE UNIVERSITY RESEARCH FOUNDATION
COLUMBUS 12, OHIO

Sponsor	U.S. Navy Purchasing Office 929 South Broadway Box 5090 Metropolitan Station Los Angeles 55, California
Contract	N123(953)-31663A
Investigation of	Study Program Related to Shipboard Antenna System Environment
Subject of Report	Final Report 7 September 1962 to 6 September 1963
Submitted by	Antenna Laboratory Department of Electrical Engineering
Date	6 September 1963

TABLE OF CONTENTS

REPORTS PUBLISHED UNDER CONTRACT N123(953)-31663A

1522-1	Tai, C. T., "On the Optimum Gain of Uniformly Spaced Arrays of Isotropic Sources or Dipoles," 31 March 1963
1522-2	Tai, C. T., "The Gain of Uniform Arrays of Isotropic Sources and Dipoles," 31 March 1963
1522-3	Interim Engineering Report, 1 June 1963
1522-4	Svoboda, D. E., "A Phase-Locked Receiving Array for High-Frequency Communication Use," 15 August 1963
1522-5	Campbell, J. T., "A Servo-Controlled Nulling System for Reducing Radio Frequency Interference," 23 August 1963
1522-6	Final Report, 6 September 1963

FINAL REPORT

I. INTRODUCTION

This final report is a summary of work performed between 7 September 1962 and 7 September 1963 on the problems of shipboard radio interference and its reduction by antenna techniques.

A serious shipboard problem is that of receiving weak signals while near-by antennas aboard the same vessel are transmitting at high power levels and coupling interference into the receiving system. One research approach to alleviate this situation has been directed toward examining antennas which would be inherently decoupled, such as traveling-wave antennas. A second approach has been to find an analytical formulation for the shipboard coupling problem from field theory; this has led, among other results, to a technique for measuring the coupling between many antennas simultaneously which appears very promising. A third approach has been the introduction of a nulling signal to cancel the interference signal; this also shows considerable promise.

Another problem arises when signals so weak compared to atmospheric noise are received that an antenna with considerable directivity is required. Because the ship may maneuver on course or swing at anchor, it is necessary to swing the directional pattern with respect to the ship. Because of the limited space aboard ship, it is difficult to construct MF and HF antennas with much directivity, and it is not possible, with present equipments, to swing the pattern. To solve this difficulty, we have investigated the use of adaptively phase-locked arrays which have the property of swinging the pattern automatically and electronically. The subject of optimum-gain arrays has also received attention, mainly to give insight into how much directivity can reasonably be expected from the limited space available aboard ship.

The problem of antenna decoupling on shipboard is a difficult one. The order of decoupling required is, in some cases, as high as 120 db. Because it is unlikely that such figures can be achieved by any one technique, several approaches were investigated during the period of this contract. Hopefully, these could be combined to satisfy the requirements.

Decoupling techniques may be broadly divided into two catagories – interior techniques and exterior techniques. The first catagory includes any device or system located behind the antenna terminals, which acts upon the incoming signal to sift it out from unwanted noise and interference. Such devices as frequency filters, nulling loops, exotic detectors (e. g., those utilizing correlation techniques) linear amplifiers, bridge circuits, etc., fall in this category. They are essentially circuit devices, which offer the advantage that they act upon the entire signal after it has been confined to a well-controlled, easily managed region within the transmission line. The second catagory includes any device or system located ahead of the antenna terminals, which presents only desired signals at the respective terminals. Such devices may comprise the antennas themselves or their judicious location and orientation; for example, the polarization characteristics, the type (travelling wave or standing wave), the spacing, the relation to nearby obstacles, the feed, all these are potential tools for decoupling in the exterior region.

It seems plausible that, in general, the greatest decoupling effect can be achieved where the decoupling action takes place in a small, high field-density region of space rather than where such action is integrated over a large volume; furthermore, dealing with such confined regions assures better reliability since there is less influence of sea motion, antenna and superstructure motion, and all other uncontrollable motions, all of which become part of the system in the exterior region. On the other extreme, however, the more confined the region of decoupling action, the more caution must be taken to assure stability because small changes effect large perturbations. Up to a point such stability should be easier to achieve for small regions.

During the past year three decoupling techniques were investigated – covering the spectrum from the interior, confined type to the exterior, diffuse type. On the one extreme, a servo-controlled nulling loop system was devised and a prototype constructed. It indicates that this method works in principle but that certain deficiencies must be corrected before it can be called feasible. These include the effects of modulation sidebands on the nulled signal and the effect of two closely spaced, interfering carriers. At the other extreme is the normal mode approach which views the entire ship and its environment as a network supporting modes which are orthogonal to one another. Progress in this area has been mostly in the form of short excursions into various approaches to determine a sound direction of attack on the problem. We feel that we now have a method based on sound principles to aid this study. Between the two extremes just mentioned, the third decoupling technique investigated was the design of multiport antennas to exhibit low coupling among the ports. The guiding

principle used here was the travelling-wave phenomenon and three antennas operating on this principle were investigated – the helix, the scimitar, and the conical spiral. Indications are that decoupling can be achieved, but that pattern deterioration is severe and coupling through feed regions is serious.

In addition, work was performed during the past year which was only obliquely directed at the decoupling problem. One effort was the design and construction of a prototype phase-locked array for r.f. operation. The results achieved with this array are promising but not yet complete. In particular, the effects of monochromatic, coherent, partially coherent, and incoherent noise must be studied both theoretically and experimentally before the array can be recommended for shipboard use. Another effort was purely theoretical research into the optimization of gain for uniformly spaced arrays. A small experimental program is associated with this work to learn how far gain optimization can be pushed before it becomes impractical. In addition, at the writing of this report, a comprehensive table of computer results is being constructed, giving the effects on small antennas of nearby conducting circular rods. Another effort was the search for a convenient experimental technique to determine the coupling between the terminals of an n-port network; although we were not able to achieve this, the work did result in some interesting graphical constructions for two-port networks.

II. ARRAY STUDIES

Antenna array studies under this contract have proceeded in three directions, each one with shipboard operation in mind. The first is a phase-locked array implemented for H. F. reception; the second is a theoretical and experimental study of optimum-gain arrays; and the third is an experimental program to develop a compact multi-antenna structure which exhibits low coupling between its several terminals and maintains good radiation pattern characteristics over a reasonable part of the 2-30 Mc band. Each of these is discussed briefly in this section.

A. Phase Locked Array Implementation for H. F. Reception

The advantages of directive antennas for distant communication purposes are obvious; they provide higher gain in the section of interest and reduce noise and interference arriving from other directions. On board ship, however, it is difficult to achieve high gains at communication frequencies due to the space limitations, especially if the antennas are to be steerable ones. Under this contract an antenna array was devised which provides a maximum gain in the direction of a distant source by

properly phasing all the array elements. Since this phasing is achieved automatically, the direction of maximum gain is always coincident with that of the source, i.e., it "tracks" the source even during ship maneuvers and sea motions. In addition, the array may be implemented to operate in a scan mode as directed by a preselected computer program. Although the array has been constructed only to receive, it is possible to instrument it for transmitting capability also. A short description of this work follows; a more detailed description may be found in Report 1522-4, "A Phase-Locked Receiving Array for High Frequency Communications Use".

An investigation was undertaken to determine the feasibility of automatically phasing a receiving array by combining the signals from each element at an intermediate frequency. This type of array not only can track a signal source automatically but it can also correct for phase errors due to individual antenna element motion, near field obstructions, and phase instabilities of electronic components. The array has essentially the pattern of a conventional program-phased array and rejects interfering signals accordingly.

A block diagram of a prototype six-element phase- locked array was constructed for experimental purposes and is shown in Fig. 1. This array can be extended to any number of elements. The received signal consists of a carrier or pilot carrier and information sidebands. The first local oscillator is tuned to adjust the operating frequency of the array. A part of the signal appearing in the second I. F. amplifier of each channel is sent to a combining network. The carrier phase, at the same point, is compared with the phase of a reference oscillator which is common to all channels and the phase-error information obtained is used to control the phase of the voltage-controlled second local oscillator. Thus, the phases of the carriers from each channel appearing at the combining point are automatically adjusted to be the same as that of the reference oscillator. A narrow-band filter is used before the phase detector to select the carrier and to eliminate much of the noise and interference which could be present in the information passband, which would otherwise disturb the automatic phasing operation. Provisions can be made for automatic amplitude control by using coherent detectors to measure carrier strength. In addition, the array may be operated in a program-phased mode by using program-phased second local oscillators instead of voltage-controlled oscillators.

A potential disadvantage of the array is that interference and noise can affect its performance by disturbing the automatic phasing process. In particular, it has been shown that an interfering signal of nearly the

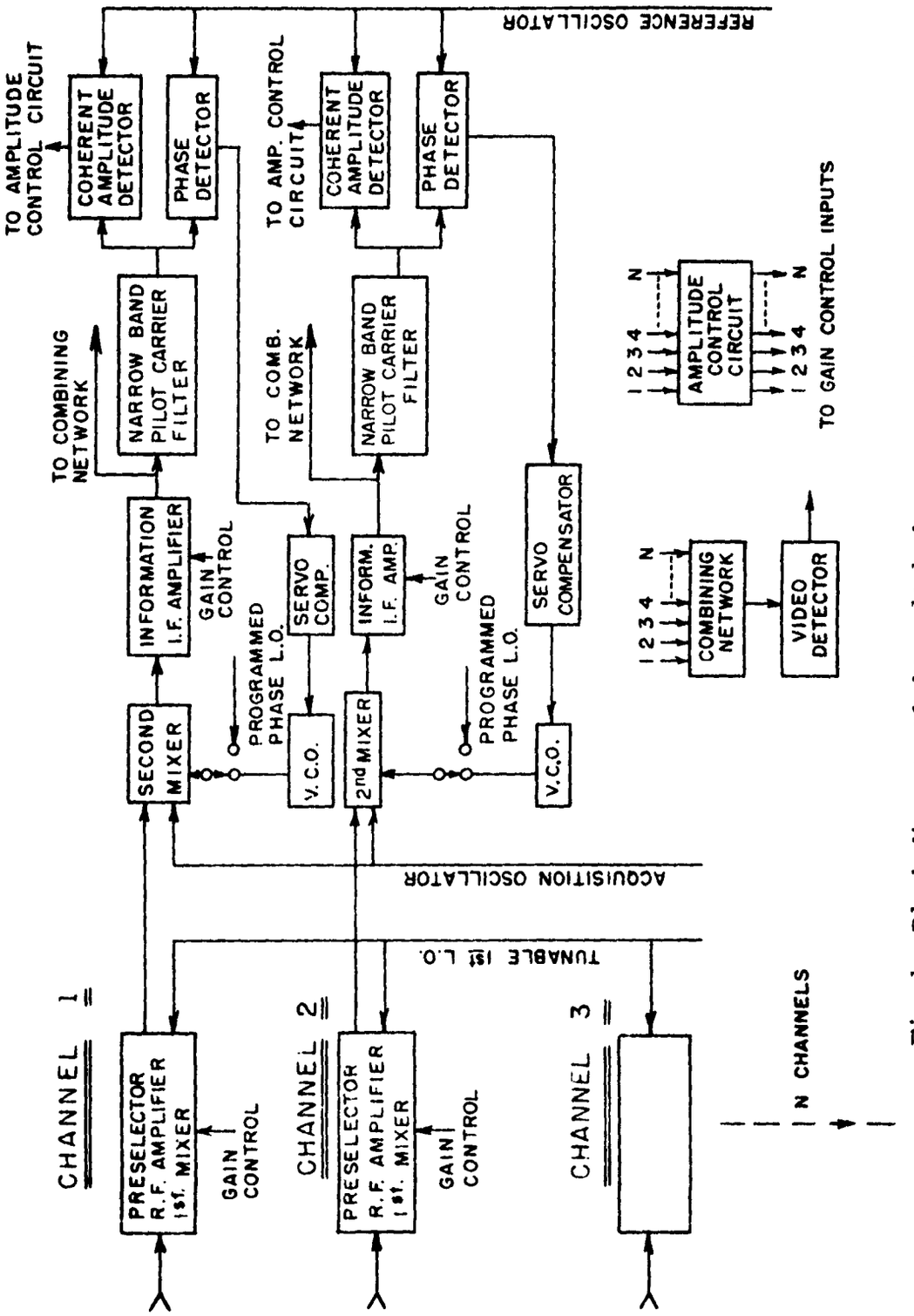

Fig. 1. Block diagram of phase-locked array prototype.

frequency as the desired signal can cause amplitude and phase modulation of the desired signal. It is recommended that theoretical and experimental work be continued to determine the effects of interference and noise of phase-locked array performance and to explore methods of eliminating these effects.

B. Optimum-Gain Arrays

For communication purposes, the optimization of the signal-to-noise ratio is the single most important consideration. But because this parameter depends so heavily upon the location and type of noise and interference sources it is not always possible to achieve its optimization. Under this contract, the optimization of the directivity of equi-spaced antenna arrays was considered instead, both to observe the effect of element spacing and to learn more about the practical minimum limits of this spacing.

The optimum directivity of various arrays of equi-spaced dipoles has been investigated theoretically as described in technical reports 1522-1, "On the Optimum Gain of Uniformly Spaced Arrays of Isotropic Sources or Dipoles", and 1522-2, "The Gain of Uniform Arrays of isotropic Sources and Dipoles". The first report deals with the general theory and the second tabulates the nominal directivity of uniformly excited arrays. It is shown in Report 1522-1 that for broadside arrays with an element spacing greater than $\lambda/2$, or for end-fire arrays with element spacing greater than $\lambda/4$, the optimum directivity and the nominal directivity do not differ significantly. The uniform array, as far as directivity is concerned, is therefore an excellent one provided that the element spacing lies beyond these critical ranges.

Experimental work is now in progress to verify, (1) the best element spacing for uniform arrays, and (2) the practical limitation in designing an optimum array with small element spacing. Initial experimental work on the optimum-gain array was concerned primarily with the problem of coupling between the array elements. An array consisting of four helices, three at the apices of an equilateral triangle, the fourth at its geometric center, was chosed as a test case. It was verified that the effects of coupling between elements on the input impedance is very small, i.e., the impedance seen at the terminals of one element is relatively unaffected by changes of termination on the remaining elements. Figures 2 and 3 present the power coupling between two helical elements as a function of feed orientations and element spacing. We note that there is a definite influence of the ground plane and helix orientation upon power coupling, a fact which can limit the utility of the helix in a ship environment.

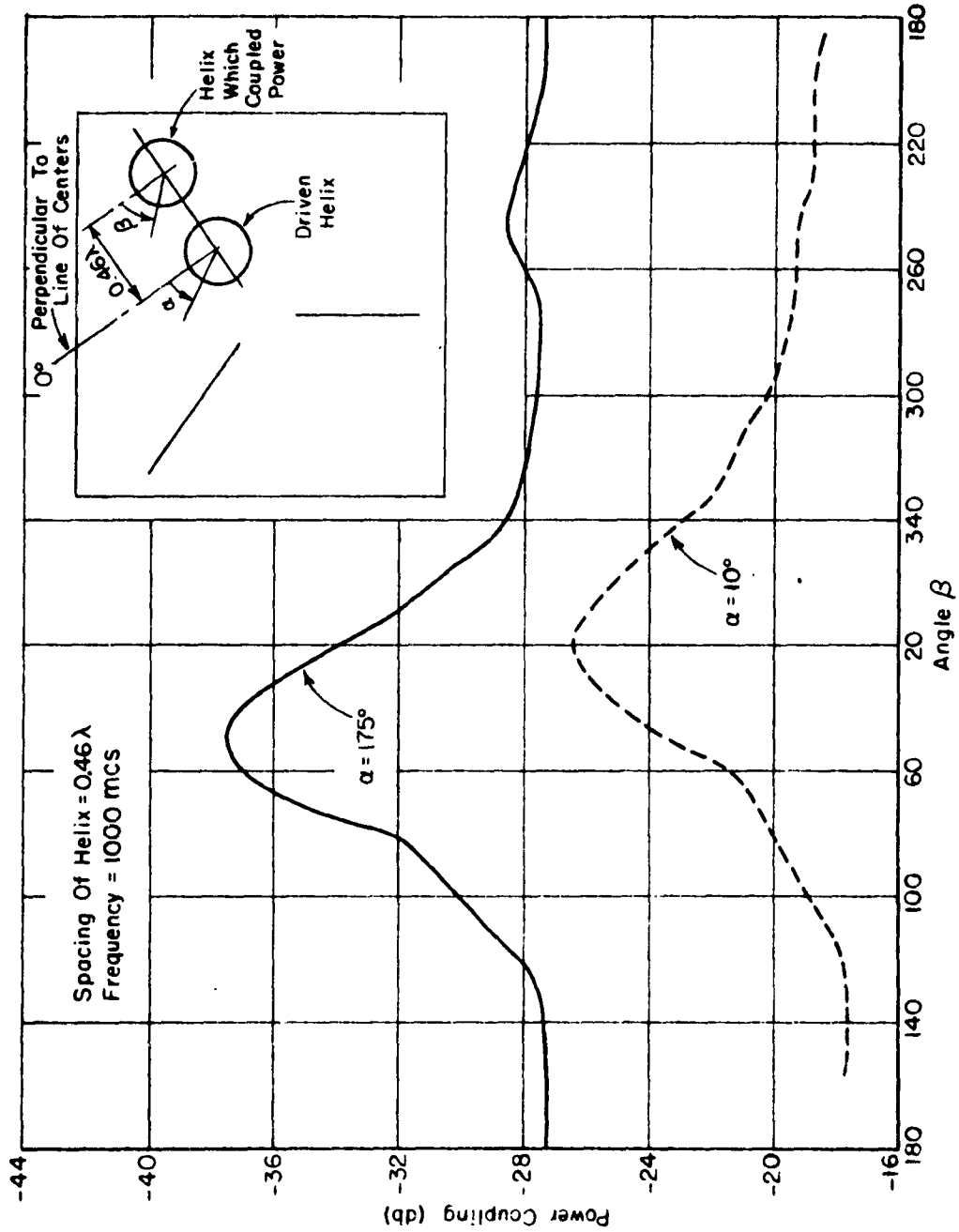

Fig. 2. Coupling between helices as a function of angle β.

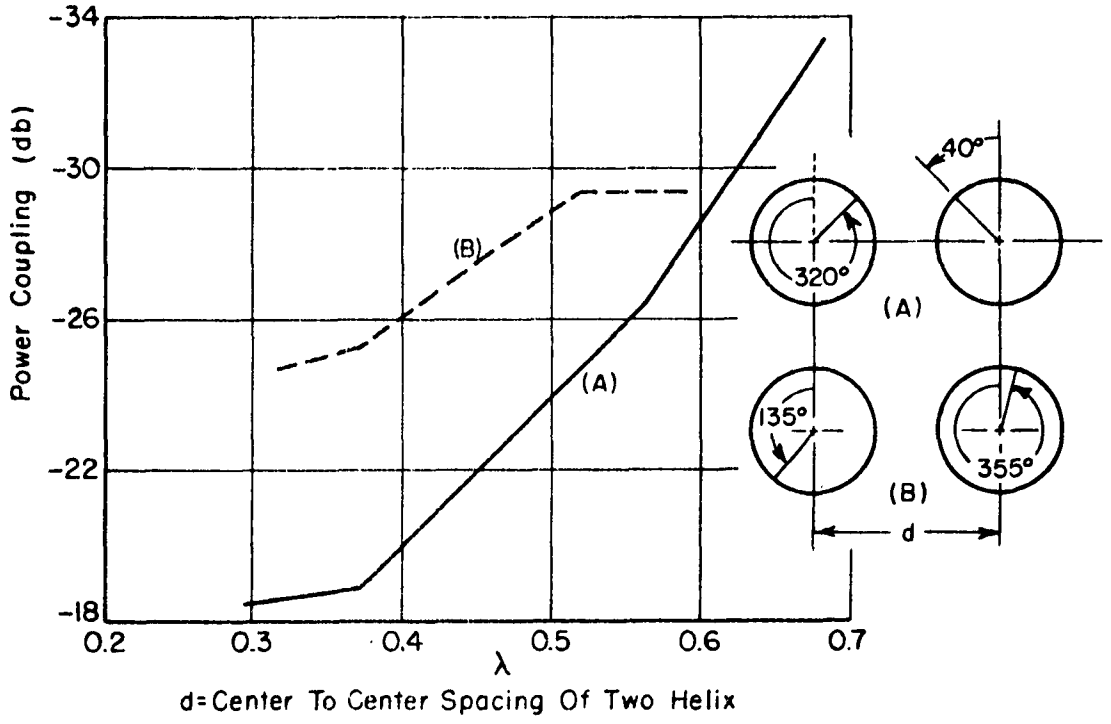

Fig. 3. Coupling between helices as a function of spacing d.

To study the interference of cylindrical conducting posts on the radiation pattern of short dipoles, an extensive calculation is being done for cylinders of various diameters, and for different orientations of the dipole as well as its separation from the cylinder. This geometry would simulate, for example, a whip antenna located near a stack. This problem has been studied previously by Carter, Lucke, Wait, and others. We hope to compile a complete set of data covering all different cases since this configuration may also approximate an interfering superstructure, guy wires, masts, etc., on shipboard.

C. Low-Coupling Antennas

Because of the large number of radiating elements that must exist on a communications ship, interaction between elements can seriously limit the capabilities of the antenna system. Conventional stub-type radiating elements exhibit high coupling. A generator at antenna A in Fig. 4 will produce a relatively large signal at the terminals of B. Kilowatts of signal at A may produce volts of signal at B for parallel stub- and dipole-type antenna elements. That is, coupling may be on the order of 10 to 20 db.

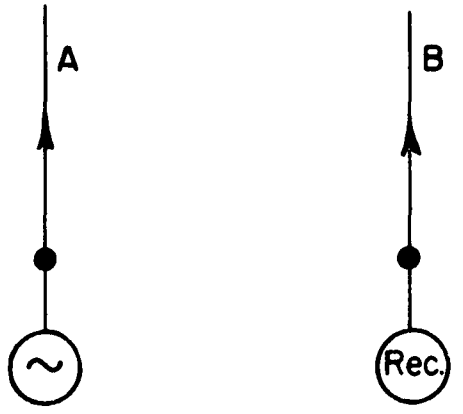

Fig. 4. Two parallel antennas.

In an attempt to reduce coupling between elements, a study has been made of some traveling-wave antenna types. If A and B in Fig. 4 are travelling wave antennas effectively terminated in matched loads, a pure travelling wave in the direction of the arrow in element A will produce a wave in the same direction in B. Ideally there is no signal coupled to the input terminals (the receiver) of element B. In practice, some discontinuity at the input to the antenna, improper termination, and scattering from surrounding structures will produce a small backward travelling wave on element B due to element A.

Antenna types that have been studied are the helix, the scimitar and the conical spiral. The helix and scimitar were described in Report 1522-3, the interim report on this contract. Coupling data for helices have been given in the previous section.

The scimitar lends itself to an antenna complex in the form of a fountain array as shown in Fig. 5. Dimensions of the L (large) and S (small) scimitars are given in Fig. 6. Coupling data comparing the scimitars with stubs of the same height are given in Table I. Column (a) is for stubs at the same locations as the scimitar feed points. Column (b) is for stub locations at the center of the scimitars. Element 1 was the fed element for the data in Table I. That is, a transmitter was connected to element 1 and the transmitted power was monitored. The db-coupling columns give the received power at individual elements in db below the transmitted power.

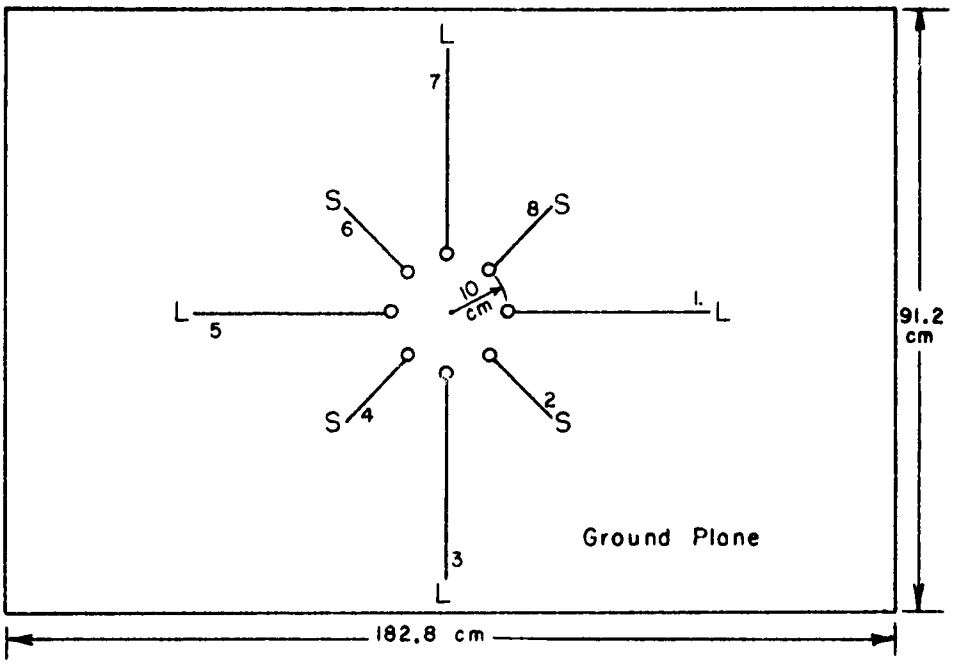

Fig. 5. Top view showing locations of scimitar antennas on ground plane.

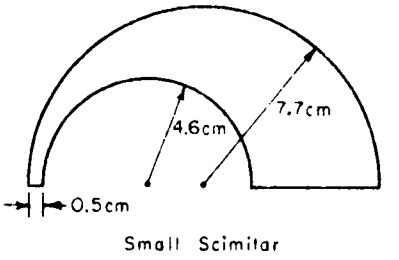

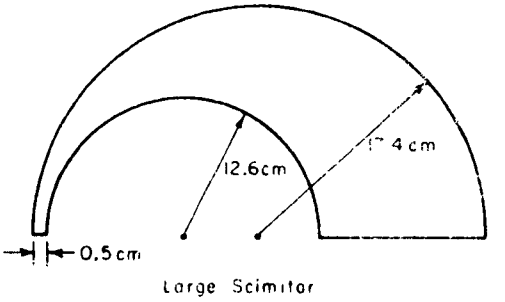

Fig. 6. Dimensions of scimitar antennas.

TABLE I

Frequency	Element Number	Coupling in db with respect to No. 1 element		
		Scimiter	stubs (a)	stubs (b)
1000 mc	8	23	15	24
"	7	27	22	28
"	6	29	28	28
"	5	29	27	36
700 mc	8	15	11	21
"	7	28	15	23
"	6	33	19	26
"	5	33	20	26
300 mc	8	20	25	24
"	7	26	36	27
"	6	26	32	28
"	5	28	33	35

A comparison of stub and scimitar patterns are shown in Fig. 7 for the first two elements of the circular array. Due to symmetry, the patterns of other elements are about the same except for rotation. Figure 7 indicates that a small scimitar fed between two large scimitars essentially forms a corner reflector antenna. The directional characteristics of such an array might be quite useful in some beam-forming applications.

Although the scimitar array exhibits somewhat lower coupling than the stub array over portions of the frequency band, these results indicate that there is no outstanding improvement in coupling to be obtained by an array of scimitars. Although impedance measurements were not made, the scimitar does have a better impedance-versus-frequency characteristic than a stub of the same height.

Another travelling-wave antenna type that has been studied is the conical spiral as illustrated in Fig. 8. This is a circularly-polarized backward-wave antenna usually utilizing one pair of spiral elements. If the two elements of the pair are fed out-of-phase the "axial mode" beam of Fig. 8(a) results. If the elements are fed in-phase the "normal

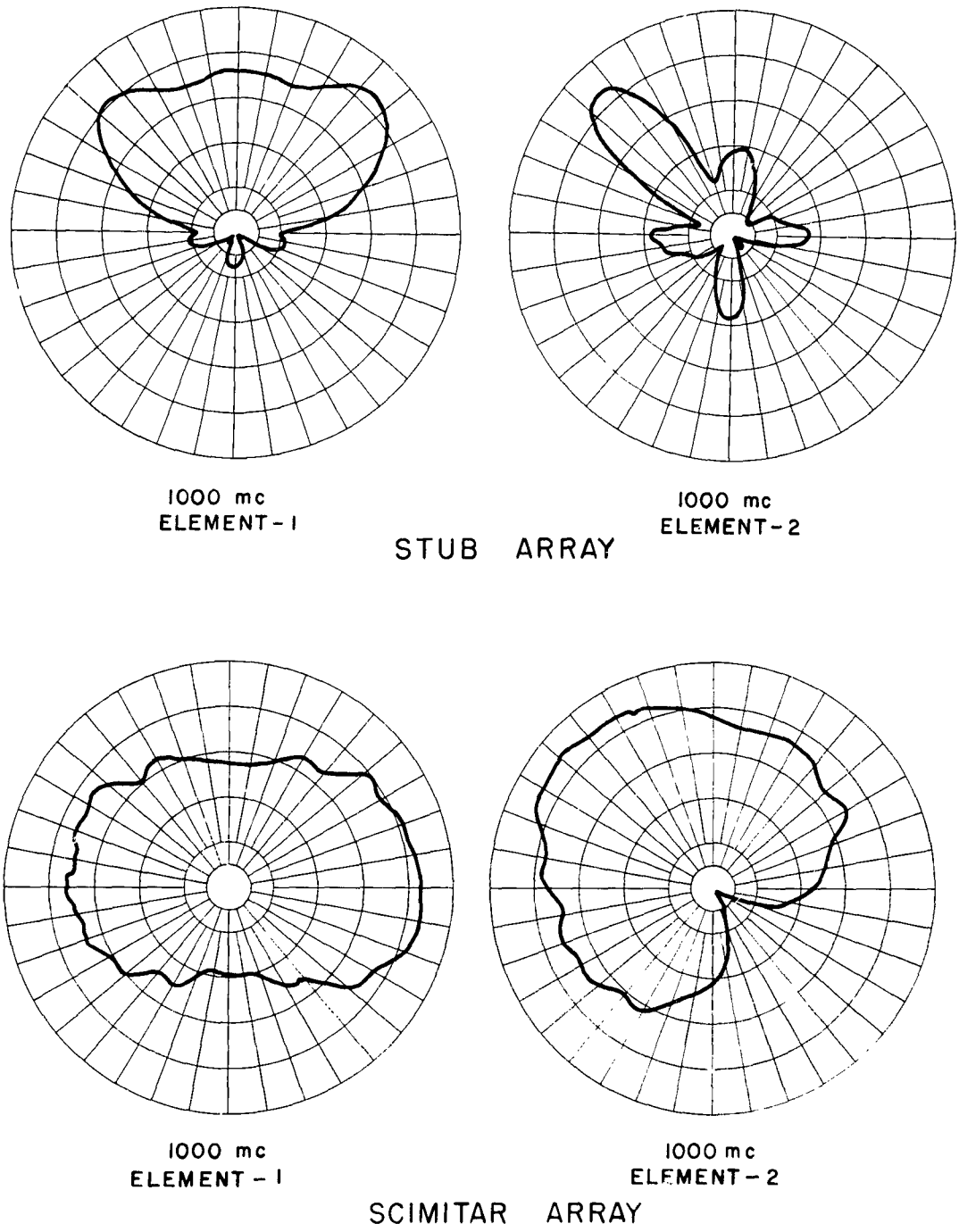

Fig. 7. Comparison of patterns of scimitar and stub arrays. Stubs located at scimitar feed points.

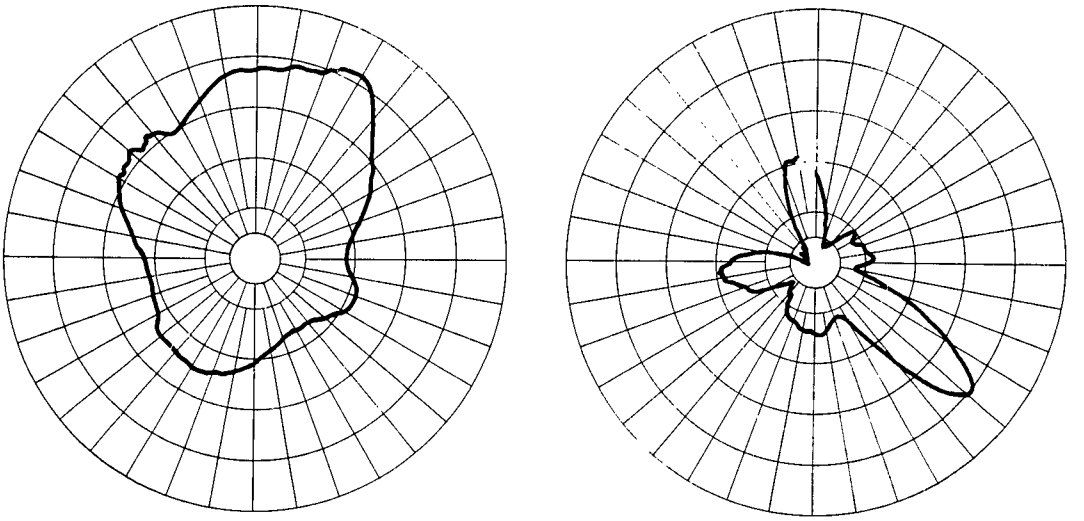

300 mc
ELEMENT-1

300 mc
ELEMENT-2

STUB ARRAY

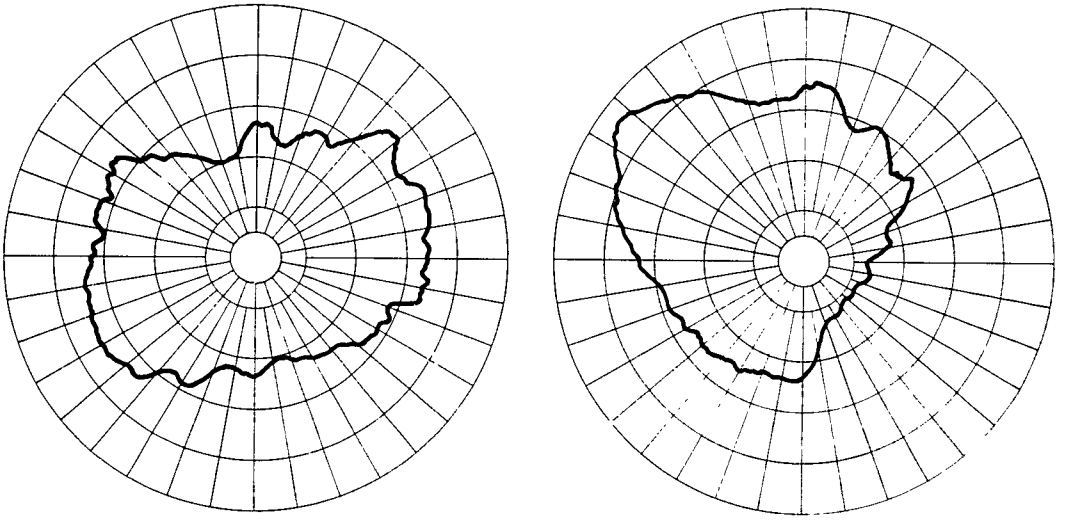

300 mc
ELEMENT-1

300 mc
ELEMENT-2

SCIMITAR ARRAY

Fig. 7.

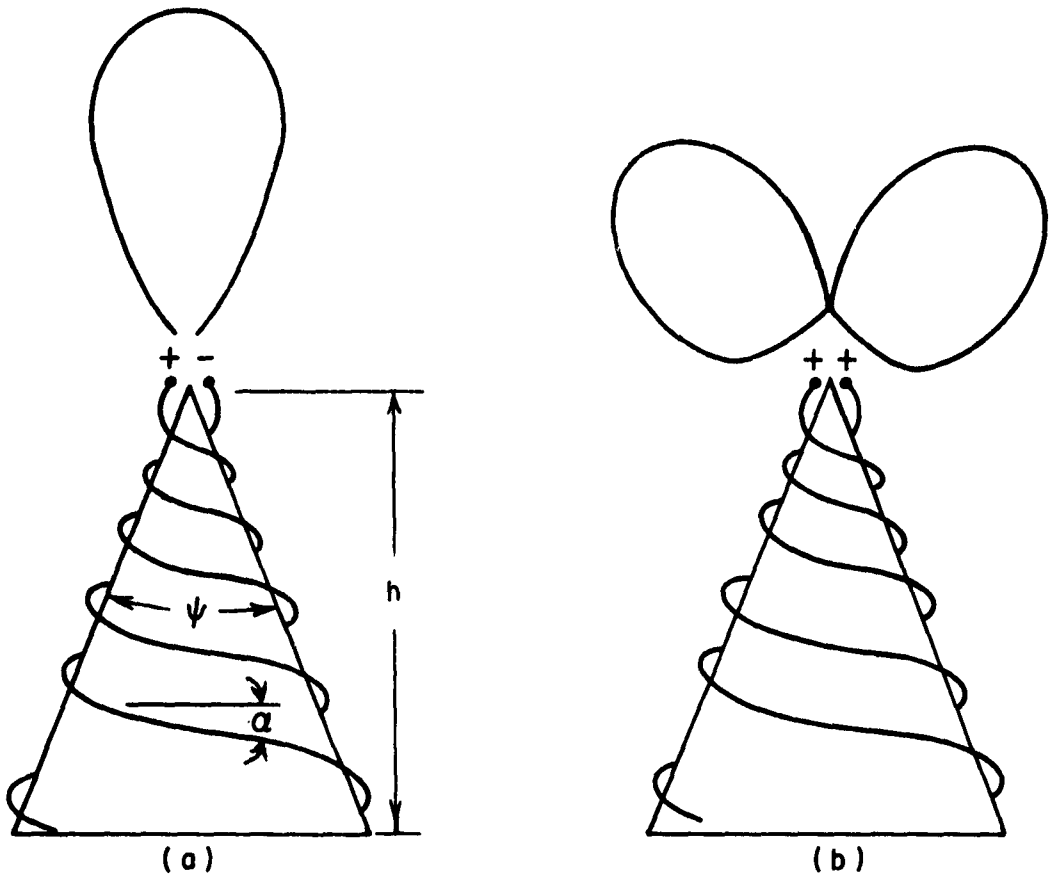

Fig. 8. Conical spiral antennas.

mode" doughnut beam of Fig. 8(b) results.[1] For shipboard use, where horizontal coverage is desired, the decision was made to study a multiple-element spiral antenna with normal-mode operation.

The feed arrangement is shown in Fig. 9. One arm of each pair is a coaxial line feeding the pair above. This type of feed is balanced in the sense that equal currents are set up on the elements. This feed arrangement requires one more pair of spiral elements than antenna terminals. An objective would be to see how many separate antennas can be operated on the same structure and still maintain good patterns with adequate decoupling between antennas.

Patterns over a band of frequencies for a one-port conical spiral are given in Fig. 10. This illustrates the normal-mode operation.

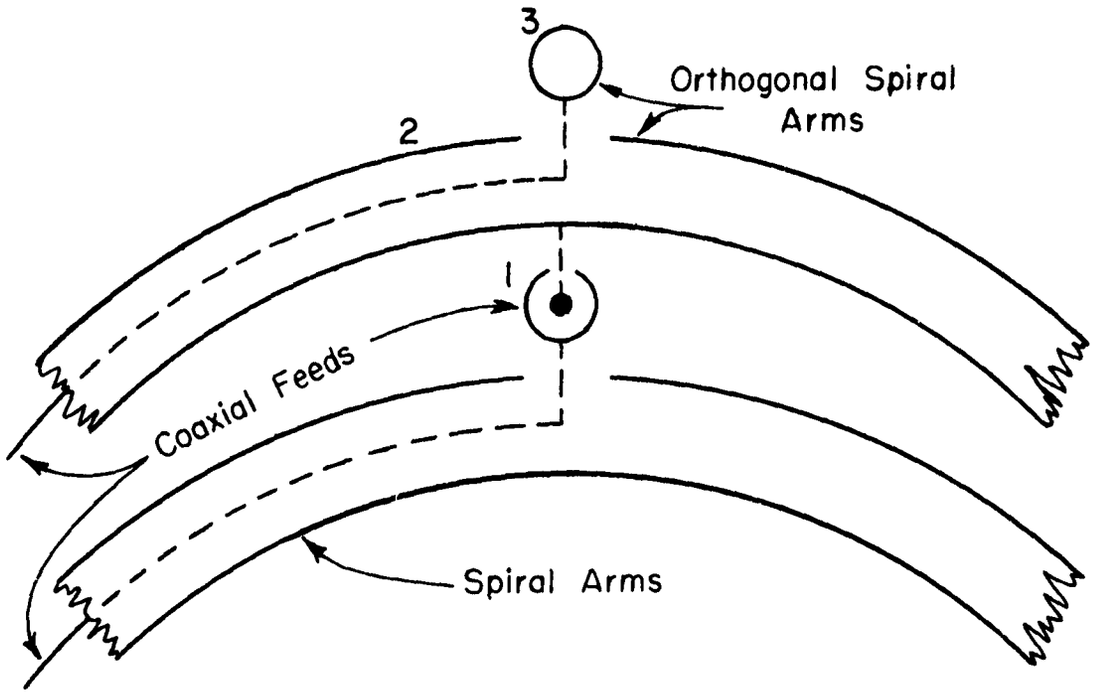

Fig. 9. Balanced feeds for in-phase excitation of spiral elements in a multiple-element structure. Figure shows a 3-port antenna.

Patterns of a three-port conical spiral are shown in Fig. 11 and measured results of coupling between ports are given in Table II.

TABLE II

Frequency	Spiral pair number	Coupling in db below pair No. 1
1000	2	9
"	3	26
700	2	7
"	3	21
300	2	11
"	3	36

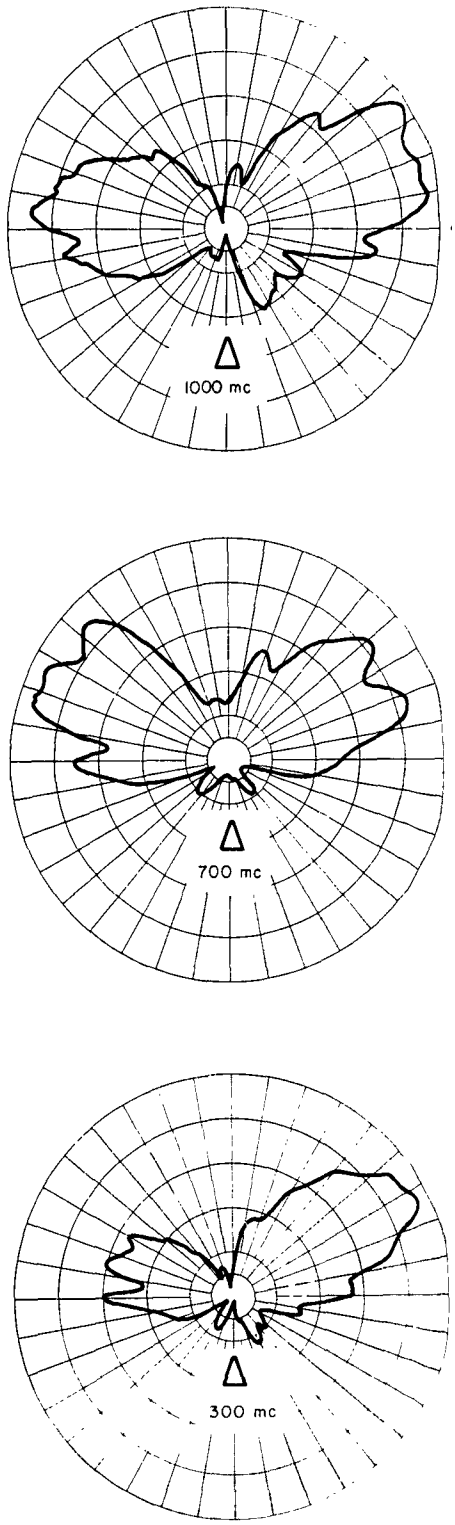

Fig. 10. Measured vertically polarized patterns of a single port conical spiral antenna (h=4.5', ψ= 20°, α=30°).

Although the patterns in Fig. 11 of the multiport conical spiral have poor sidelobes and tend to be asymmetrical, this appears to be due to the feed construction which was somewhat crude in the model that was tested. The results indicate that with careful design of the feed section a multiple port conical spiral can give good patterns over better than a 2:1 band of frequencies and with quite low coupling between some of the ports.

III. REDUCTION OF INTERCHANNEL INTERFERENCE BY SERVO-CONTROLLED NULLING LOOP

The presence of several high-powered transmitters in the vicinity of an antenna attempting to receive a weak, distant signal at frequencies that are near or even coincident is typical of a shipboard environment. Hundreds of volts of interfering signal can be induced at the receiver terminals alone with mullivolts of desired signal. If the desired and interfering signals are suitably separated in frequency, filtering may alleviate much of the problem but where these frequencies coincide filtering is ineffective. For this reason, and to complement Navy Electronics Laboratory's own extensive filter research program, effort during this contract period was directed at a servo controlled nulling system. Such a system accepts the fact that a transmitter, T_1, at frequency f_1, will induce a large voltage at receiver terminals R by coupling paths in the exterior region but it provides an additional path in the form of a transmission line between T_1 and R; the signal coming via this interior path can be controlled accurately in phase and amplitude to cancel that coming via the exterior path. To ensure that the cancellation is continuous and independent of changes in the exterior path, the attenuator and phase shifter in this so-called "nulling loop" are servo-controlled. If a second transmitter T_2 at frequency f_2 is offending the receiver R, in the same way a second loop can be devised to cancel its interference. By building up a sequence of such loops, a master switchboard can be envisioned which will ensure that nulling loops are connected between all transmitters which are offending one or several receivers during simultaneous operation.

During the past year a study was made to establish the feasibility of a servo-controlled nulling loop between a single transmitter channel and a single receiver channel in order to reduce extreme R. F. interference between them. A complete description of this work is given in Technical Report 1522-5, "A Servo-Controlled Nulling System for Reducing Radio Frequency Interference". An experimental prototype designed to cancel a low-level 4.5 mc signal is described, including verification of the predicted error voltages, measurement of the servo-system response, and measurement of null depth as a function of

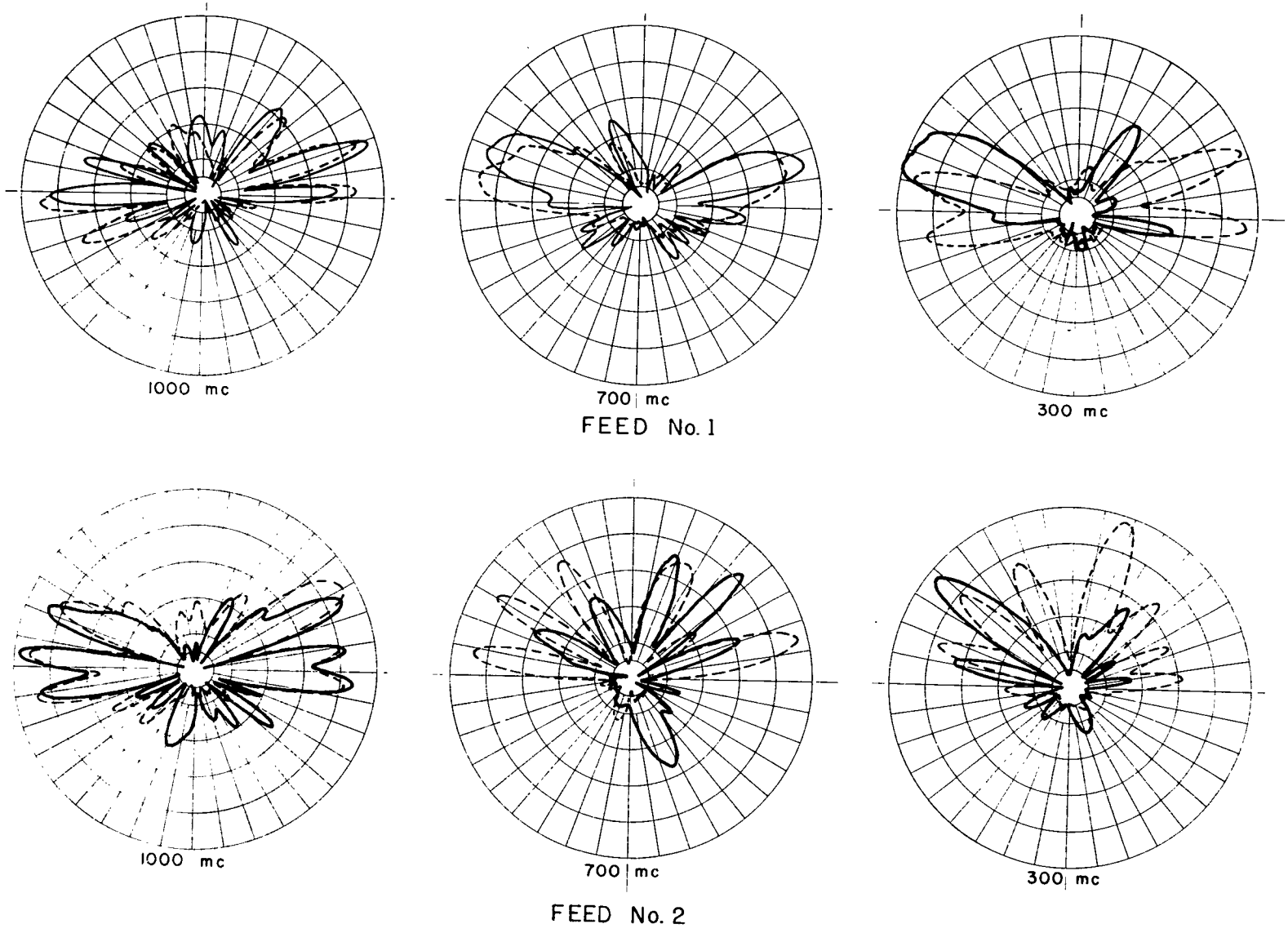

Fig. 11. Measured patterns of a 3-port conical spiral antenna ($h=4.5'$, $\psi=20^{\circ}$, $\alpha=30^{\circ}$). Dashed lines correspond to vertical polarization, solid lines correspond to horizontal polarization.

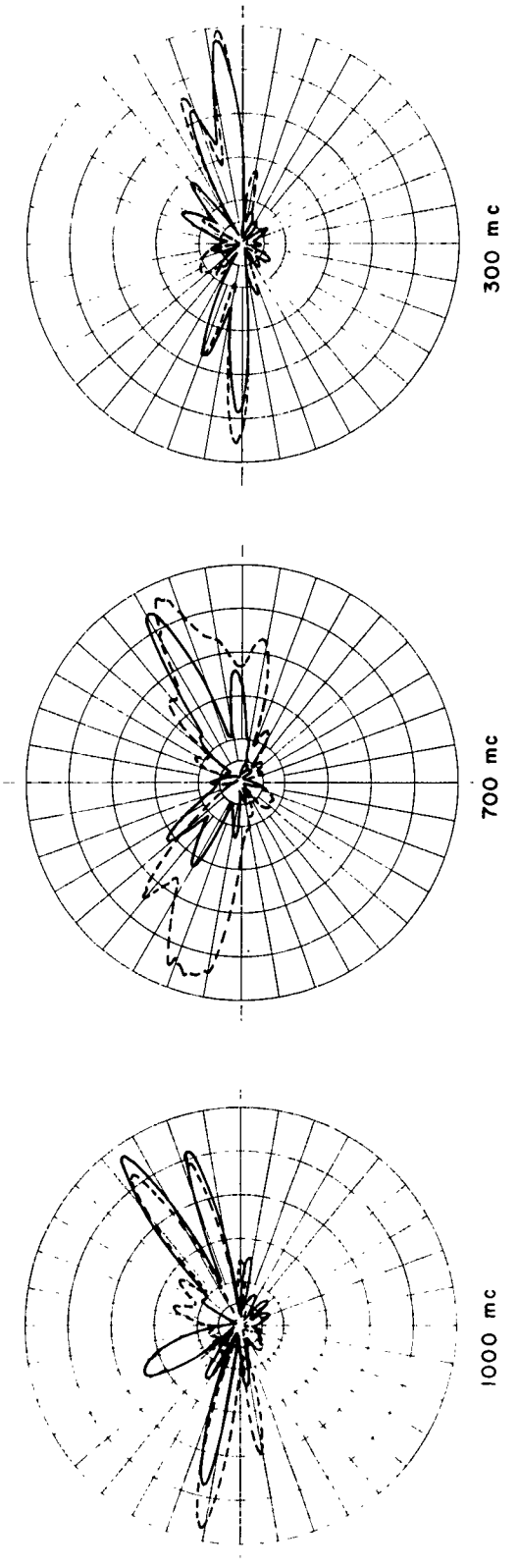

Fig. 11.

interfering signal strength. On the basis of analytical and experimental results, the following conclusions are drawn:

(1) Nulls in excess of 45 db can be expected for a cw interference signal.

(2) No severe limitations exist which preclude the operation of a servo-controlled nulling system at high power levels.

(3) The system can be expected to automatically cancel AM as well as cw interfering signals.

Questions which remain to be answered are: how close in frequency can two interfering signals lie and still be nulled to better than 45 db by associated nulling loops? Is there a serious degradation of nulling loop performance due to motion of the antenna elements and vibration effects on narrow-band filters in the system? How does multi-path coupling in the exterior region influence the nulling capability?

IV. FIELD METHODS FOR ANTENNA DECOUPLING

By field methods for antenna decoupling, we mean the excitation of the fields and currents in the surrounding environment of the antennas such that the antenna ports are decoupled. Such decoupling via field configurations are not unusual in closed systems, e.g., the matched hybrid tee in waveguide, but they are less common in radiating systems. We have called the field configurations which are effectively decoupled from one another "normal modes", and though these normal modes are founded soundly in theory, it is not clear how to approach them in practice. Some preliminary work with thin wires, both finite and infinite, indicated that the concept of normal modes for radiating and scattering bodies was worth further investigation. However, the methods used in the study of thin wires were cumbersome and unsuited for the real case of interest, that of three dimensional bodies. Recently several new approaches have been devised to study normal modes in the three dimensional case and these are being used as described in the Appendix. In particular, rectilinear and cylindrical bodies have been chosen as test objects since two separate approaches may be applied to them and then compared. No results are available yet.

Another effort which is described in detail in the Appendix was an attempt to devise an experimental technique to help decouple a set of antennas. The aim was a visual presentation of the relative couplings

among all the antennas simultaneously even as they were being moved about a model to satisfy some minimum coupling criterion. A method involving the use of square-wave modulated diodes as loads on all but the excited antenna was studied but it was found that too much information about the antenna impedances was needed to make it practical. Subsidiary to this work was the development of interesting graphical tools for use with lossless two-port networks. This is also described in detail in the Appendix.

V. RECOMMENDATIONS

It is recommended that:

(1) The feasibility study of the servo-controlled nulling loop be continued. This will include a thorough investigation of the effects of modulation and nearby carriers and of methods to improve system performance under these conditions. Also, the response of the system to inherent phase and amplitude changes due to vibration may be investigated.

(2) The receiving characteristics of the phased array be investigated more fully, in particular under conditions of various types of interfering noise. In addition some thought should be given to implementing the array for transmitting.

(3) The normal-mode study be continued as outlined in the Appendix.

VI. BIBLIOGRAPHY

1. Dyson, J. D. and Mayes, P. E., "New Circularly-Polarized Frequency-Independent Antennas with Conical Beam or Omni-directional Patterns," IRE Trans. on Antenna and Propagation, vol. AP-9, pp. 334-342, July 1961.

2. Tsu, R., "The Theory of Application of the Scattering Matrix for Electromagnetic Waves", Report 1073-2, 1 April 1960, Antenna Laboratory, The Ohio State University Research Foundation; prepared under Contract AF 30(602)-2166, Rome Air Development Center, Griffiss Air Force Base, New York.

3. Richmond, J. H., "Reciprocity Theorems and Plane Surface Waves", Engineering Experiment Station Bulletin 176, The Ohio State University, July 1959.

4. Kennaugh, E. M., "Multipole Field Expansions and Their Use in Approximate Solutions of Electromagnetic Scattering Problems", Report 827-5, 1 November 1959, Antenna Laboratory, The Ohio State University Research Foundation; prepared under Contract AF 19(604)-3501, Air Force Cambridge Research Center, Bedford, Massachusetts.

5. Turnbull and Aitken, An Introduction to the Theory of Canonical Matrices, Blackie and Son, Limited, London and Glascow, 1932, p. 185.

6. MacDuffee, The Theory of Matrices, Chelsea Publishing Co., New York, 1956, pp. 74-78.

7. Dawirs, H. N., "Graphical Filter Analysis," IRE Transactions on Microwave Theory and Techniques, January 1955.

8. Dawirs, H. N. and Damon, E. K., "Application of The Ohio State University Filter Analysis Chart", Proc. of the National Electronic Conference, Vol. 10, February 1955.

9. Dawirs, H. N., "A Chart for Analyzing Transmission Line Filters from Input Impedance Characteristics", Proc. I. R. E., April 1955.

10. Stock, D. J. R. and Kaplan, L. J., "Non Euclidian Geometric Representations for Microwave Networks," The Microwave Journal, March, April 1962.

11. Mathis, H. F., "Still Another Method for Transforming Impedances Through Lossless Networks," IEEE Trans. on Microwave Theory and Technique, May 1963.

12. Green, R. B., "The Effect of Antenna Installations Upon the Echo Area of an Object," Report 1109-3, 29 September 1961, Antenna Laboratory, The Ohio State University Research Foundation; prepared under Contract AF 33(616)-7386, Aeronautical Systems Division, Wright-Patterson Air Force Base, Ohio.

13. Garbacz, R. J., "The Determination of Antenna Parameters by Scattering Cross-Section Measurements. I. Antenna Impedance," Report 1223-8, 30 September 1962, Antenna Laboratory, The Ohio State University Research Foundation; prepared under Contract AF 33(616)-8039, Aeronautical Systems Division, Wright-Patterson Air Force Base, Ohio.

14. Garbacz, R. J., "The Determination of Antenna Parameters by Scattering Cross-Section Measurements. II. Antenna Gain," Report 1223-9, 30 November 1962, Antenna Laboratory, The Ohio State University Research Foundation; prepared under Contract AF 33(616)-8039, Aeronautical Systems Division, Wright-Patterson Air Force Base, Ohio.

15. Garbacz, R. J., "The Determination of Antenna Parameters by Scattering Cross-Section Measurements. III. Antenna Scattering Cross Section," Report 1223-10, 30 November 1962, Antenna Laboratory, The Ohio State University Research Foundation; prepared under Contract AF 33(616)-8039, Aeronautical Systems Division, Wright-Patterson Air Force Base, Ohio.

16. Garbacz, R. J. and Eberle, J. W., "The Measurement of Time Quadrature Components of a Scattered Field," 1960 IRE WESCON Convention Record, Pt. 1.

17. Kennaugh, E. M., "Polarization Properties of Radar Reflections," Report 389-12, 1 March 1952, Antenna Laboratory, The Ohio State University Research Foundation; prepared under Contract AF 28(099)-90, Rome Air Development Center, Griffiss Air Force Base, New York.

APPENDIX
FIELD METHODS FOR ANTENNA DECOUPLING

A. The Concept of Normal Modes on a Body

When a scatterer is viewed as a multi-mode antenna, its scattering cross-section as a function of source and receiver directions can be written as

$$\sigma(\theta_s,\phi_s;\theta_r,\phi_r) = \sum_i C_i F_i(\theta_s,\phi_s) F_i(\theta_r,\phi_r)$$

where θ_s and ϕ_s are the spherical coordinates of the source and θ_r and ϕ_r are those of the receiver (both of which are remote from the target), $F_i(\theta,\phi)$ is the radiation pattern of the i^{th} mode set up on the target, and C_i is a constant associated with the termination of the i^{th} mode. We assume that the mode fields are mutually orthogonal and that only a finite number of $|C_i|$ exceed an arbitrarily chosen magnitude. For targets of maximum dimension on the order of wavelengths, this number should not exceed ten or so.

These orthogonal or "normal" modes, as we have called them, are related to the eigenvectors of the target scattering matrix and the C_i are determined from the associated eigenvalues. The mode patterns are useful for studying the radiation, receiving, and scattering characteristics of the target.

The scattering matrix of an arbitrary target is, in general, infinite in dimension and its elements must be determined by approximations and/or by experiments.[2] Since determination of the eigenvectors of this matrix can be a formidable problem, some more direct method for obtaining the normal modes of a particular shape is being sought.

Consider a cavity whose conducting walls have the shape of the target under study. At certain frequencies this cavity will exhibit resonances, that is, fields of those frequencies will be supported within the cavity volume which (assuming no losses) are self-sustaining, i.e., need no source to maintain themselves once they are set up. Next, consider that the currents induced on the interior walls of such a cavity at resonance are transferred to the exterior of the cavity and allowed to

radiate. Because these currents are associated with a resonance condition, i.e., standing waves, the reaction between them and a plane wave of the resonant frequency and incident on the target from any direction will be zero if the reaction integral is taken over a surface enclosing the cavity.[3],[4] If the current assumed is that of a normal mode for the shape under consideration, this zero reaction implies that this particular normal mode at that frequency is not excited, i.e., C_i is zero. This fact in itself is incidental; however, if we postulate that the current configuration of any one normal mode changes very little or not al all with a slight change in frequency (for example, the form of the multipole currents on a sphere are independent of frequency), then we can use this fact to evaluate a coefficient for a normal mode at a frequency slightly removed from resonance. Obviously the cavity cannot maintain fields within itself at this new frequency so the question arises, how do we arrive at a current distribution to use in the reaction integral? To do this, the cavity is filled with a material such that it resonates at the new frequency. This material can have $\epsilon_r > 1$ or $\mu_r > 1$, or both. Since resonance is maintained, the form of the wall currents will be essentially unchanged and will satisfy the boundary conditions properly. If again this current is regarded as flowing on the exterior of the cavity, the reaction integral over a surface surrounding the cavity performed with a plane wave at the new frequency has a non-zero value which is related to the coefficient C_i corresponding to a normal mode current at that frequency. This view may be supported as follows. By filling the cavity with material other than free space, we have effectively introduced a set of polarization currents within the cavity volume to maintain fields which satisfy the boundary conditions on the walls of the new frequency. These polarization currents appear as a source in the reaction formulation within the cavity volume, and in general, a reaction integral taken on a surface separating two sources is not zero. Since, in our case, this surface is that of the cavity bounding wall, the polarization current source is on one side and the plane wave source is on the opposite side, thereby causing non-zero reaction.

The methods outlined above are being applied to two simple cavity shapes which can be studied theoretically, viz, the rectilinear cavity and the cylindrical cavity. For arbitrary shapes, for which no exact theory can be found, an approach may be used in which a sufficiently large spherical cavity is excited when empty and its appropriate resonance frequencies noted. Upon introduction of a test shape into this cavity at its center, these resonant frequencies shift, but the original frequencies may be regained by increasing the cavity size. By noting the amount of increase at each resonance the assumption of a large enough cavity permits an evaluation of the phase shift between the incoming and outgoing

waves due to the test object. These phase shifts are related at each resonant frequency to normal mode coefficients. By probing the fields near the cavity walls, the corresponding normal mode patterns may be determined. The problem of devising a spherical cavity continuously variable in size over at least a wavelength in diameter is a formidable one.

B. Graphical Two-Port Techniques

This section describes several geometrical constructions on the Smith Chart which are useful in transforming impedances through lossless two-port networks. The same concepts may be extended to lossy networks by application of the Poincaré sphere.

Any linear two-port network may be represented mathematically by a two-by-two matrix, say $\overline{\overline{T}}$. Such a matrix, which is non-singular, can always be represented uniquely (if H and H' defined below are positive definite) as the product of a Hermitian matrix and a unitary matrix.[5,6] This is clear from the following development.

$$\overline{\overline{T}} = \overline{\overline{U}}\,\overline{\overline{D}}\,\overline{\overline{V}} \tag{1}$$

where $\overline{\overline{D}}$ is a real, positive diagonal matrix and $\overline{\overline{U}}$ and $\overline{\overline{V}}$ are unitary matrices.[2] Regrouping these in two ways,

$$\overline{\overline{T}} = \underbrace{\overline{\overline{U}}\,\overline{\overline{D}}\,\overline{\overline{U}}^{-1}}_{\overline{\overline{H}}}\;\underbrace{\overline{\overline{U}}\,\overline{\overline{V}}}_{\overline{\overline{R}}}\,, \tag{2}$$

or

$$\overline{\overline{T}} = \underbrace{\overline{\overline{U}}\,\overline{\overline{V}}}_{\overline{\overline{R}}}\;\underbrace{\overline{\overline{V}}^{-1}\,\overline{\overline{D}}\,\overline{\overline{V}}}_{\overline{\overline{H}}'}\,. \tag{3}$$

The $\overline{\overline{H}}$ and $\overline{\overline{H}}'$ matrices represent projective warpings of points on the Poincaré sphere into other points on the same sphere by an inversion through a point within the sphere followed by an inversion through the center of the sphere.[17] The $\overline{\overline{R}}$ matrix represents a rotation about some diameter of the sphere. Accordingly, any point on the Poincaré sphere,

representing a load impedance, may be transformed to its corresponding point on the same sphere, representing an input impedance, by an inversion operation and a rotation, or vice-versa. (Note: we shall always mean by an "inversion operation" an inversion through a point in the sphere followed by an inversion through its center, or vice-versa.) In the special case of a lossless network, the inversion point must lie in the equatorial plane and the rotation must be about the North-South polar axis because reactances must transform back into reactances (the equator). For this reason, all geometrical constructions for lossless networks may be performed in the equatorial plane, which is the Smith chart plane.

A lossless symmetrical network may be represented by a characteristic-impedance, Z_o, and a propagation factor, γ. Either characteristic impedance is pure real, in which case the propagation factor is pure imaginary and represents a phase shift, or, the characteristic impedance is pure imaginary, in which case the propagation factor is pure real and represents an attenuation.

Assume that we have such a symmetrical network with characteristic impedance, R_o, and phase factor, $j\beta$. We know that if this network is terminated in a resistance, R_o, the input impedance must also be purely resistive and equal to R_o. Hence, any geometrical construction relating load impedance and input impedance for this network must transform R_o into R_o. In this context consider Fig. 12. As stated previously, for a lossless network the inversion point must lie in the equatorial plane; to find where in the equatorial plane, we reason as follows. If R_o must transform into itself via an inversion process and a rotation about the North-South polar axis, an inversion through any point on C_1 will end on C_2, which if inverted through the center will end on C_3. A rotation of proper amount about N-S will then end at R_o as required. And since this process is unique, we say that the inversion point must lie on the circle, C_1. Note that the diameter of this circle is dependent soley on the characteristic impedance, R_o, of the network and not on its phase factor. The location of the inversion center, I, on the appropriate circle and the rotation angle, α_{rot}, is found as indicated in Fig. 13. The points OC' and SC' correspond to the input reactances with the network open circuited and short circuited respectively. It may be verified by simple trigonometry that

$$\cot \psi = \frac{1}{2}\left(\frac{R_o^2 + 1}{R_o}\right)\tan \beta \ell \ , \tag{4}$$

and

(5) $$\alpha_{rot} = \pi - 2\psi,$$

where $\beta\ell = \frac{2\pi\ell}{\lambda}$ is the phase shift through the network in radians. The radius of the circle, C_1, is

(6) $$r = \frac{1}{2}\left(\frac{R_o^2 - 1}{R_o^2 + 1}\right),$$

and the distance of I from the center is

(7) $$R = \left(\frac{R_o^2 - 1}{R_o^2 + 1}\right)\cos\psi,$$

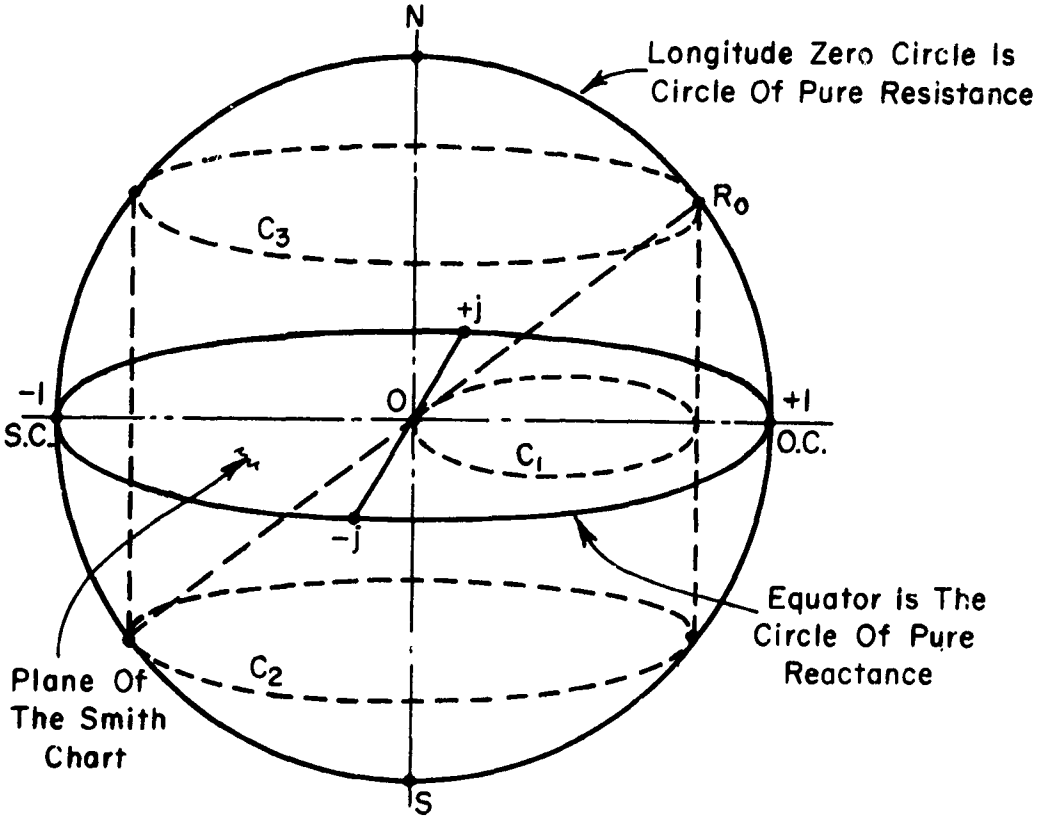

Fig. 12. A sketch of the Poincaré sphere and the construction associated with the constant impedance circle, C_1.

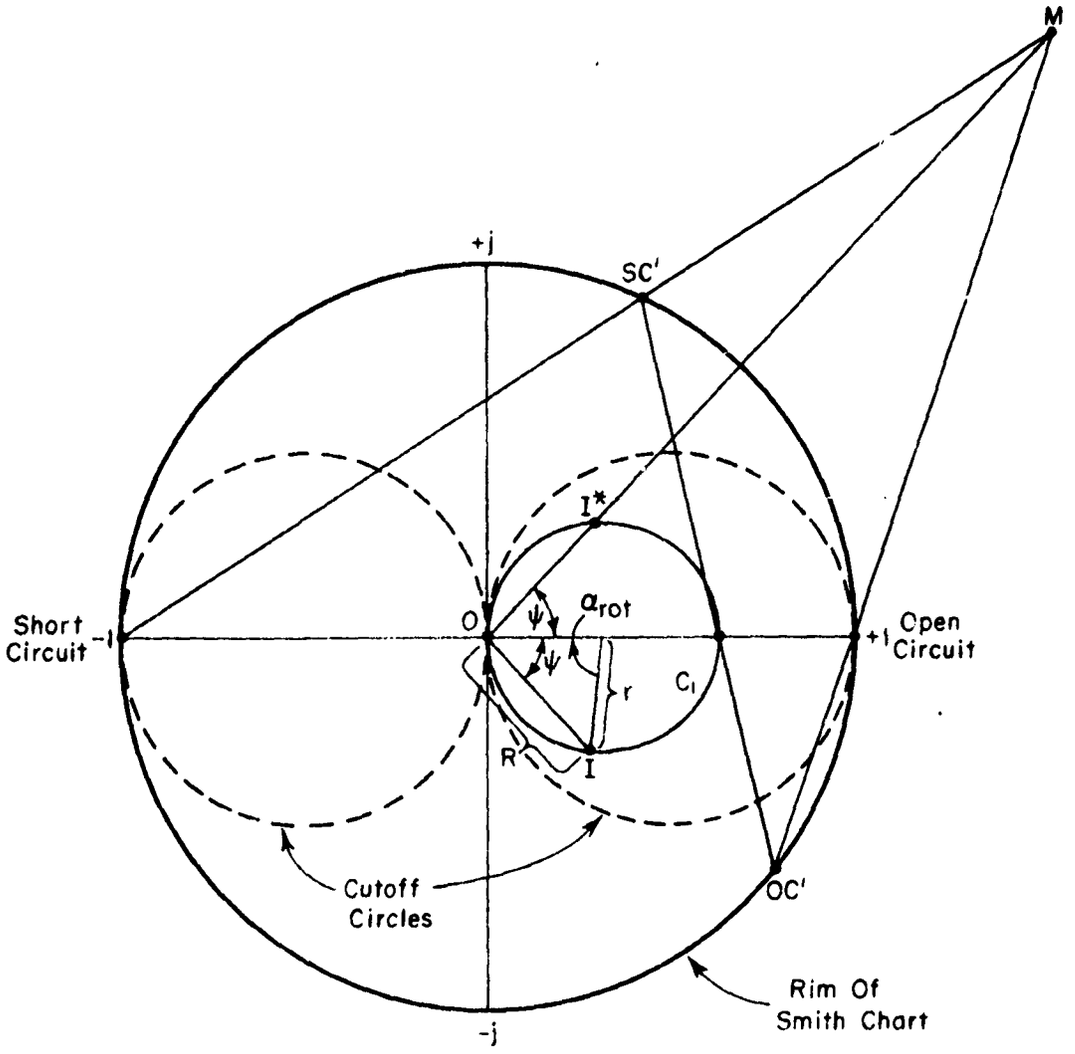

Fig. 13. Geometry in the Smith chart plane relating the inversion point and the angle of rotation.

where it is assumed that the Smith Chart has a unit radius. In the example cited above, a network was assumed which had a real characteristic impedance. We find that all such networks will have inversion points lying within the dashed circles shown in Fig. 13, called cutoff circles. If the characteristic impedance of the network is pure imaginary, the inversion point is located exactly as before but it will be found to lie outside the cutoff circles. Figure 14 shows within the unit circle (which can be thought of as superimposed on the Smith Chart) a grid of circles of constant characteristic impedance intersecting curves of constant phase shift (inside the cutoff circles) or curves of constant attenuation (outside the cutoff circles).* The intersection of a particular circle, say $R_o = 2$, with a particular curve, say, $\ell = 0.35\lambda$, corresponds to the complex conjugate of the inversion point for a network having characteristic impedance $R_o = 2$ and phase shift $\beta\ell = \frac{2\pi}{\lambda}(0.35\lambda) = 0.7\pi$ radians; the rotation angle, α_{rot}, is also indicated.

Before proceeding further, let us consider the inversion-rotation construction for the lossless, symmetric-transmission line sketched in Fig. 15. Let $Z_L = j150\,\Omega$ and arbitrarily normalize this to $R_N = 50\,\Omega$ whence $Z_L/R_N = j3$. Also $R_o/R_N = 2$, which fixes the inversion point I at the intersection of the $R_o = 2$ circle and the phase constant line $\ell = 0.50\lambda - 0.15\lambda = 0.35\lambda$ in Fig. 14. Transferring this point to a Smith Chart, Fig. 16a, we see how an inversion through I, then through 0, followed by a rotation, α_{rot}, yields the input impedance normalized to R_N. Figures 16b, c, d present alternative constructions in which these same geometric operations are used in different sequences as indicated. Such alternative constructions have advantages in certain cases as will be shown later.

A lossy load may be transformed through a lossless network as shown in Fig. 17. If the load is Z_L and the arbitrary normalizing constant is R_N, its stereographic projection onto the equatorial plane lies at the Smith chart coordinates Z_L/R_N; this is transformed into its corresponding orthographic projection via a "butterfly" diagram[10] to the point Z_L'/R_N. A line drawn through this point and the inversion center, I, cuts the unit circle at two points which fix a circle whose center is on the line. This circle can be thought of as having been rotated 90° about the line to lie in the plane of the paper for convenience; actually it represents the cross section of a slice taken through the Poincaré sphere perpendicular to the plane of

---

*This chart, called a "filter analysis chart" was developed at The Ohio State University Antenna Laboratory some time ago by Dr. H. N. Dawirs to analyze transmission line filters from their input impedance characteristics.[7,8,9]

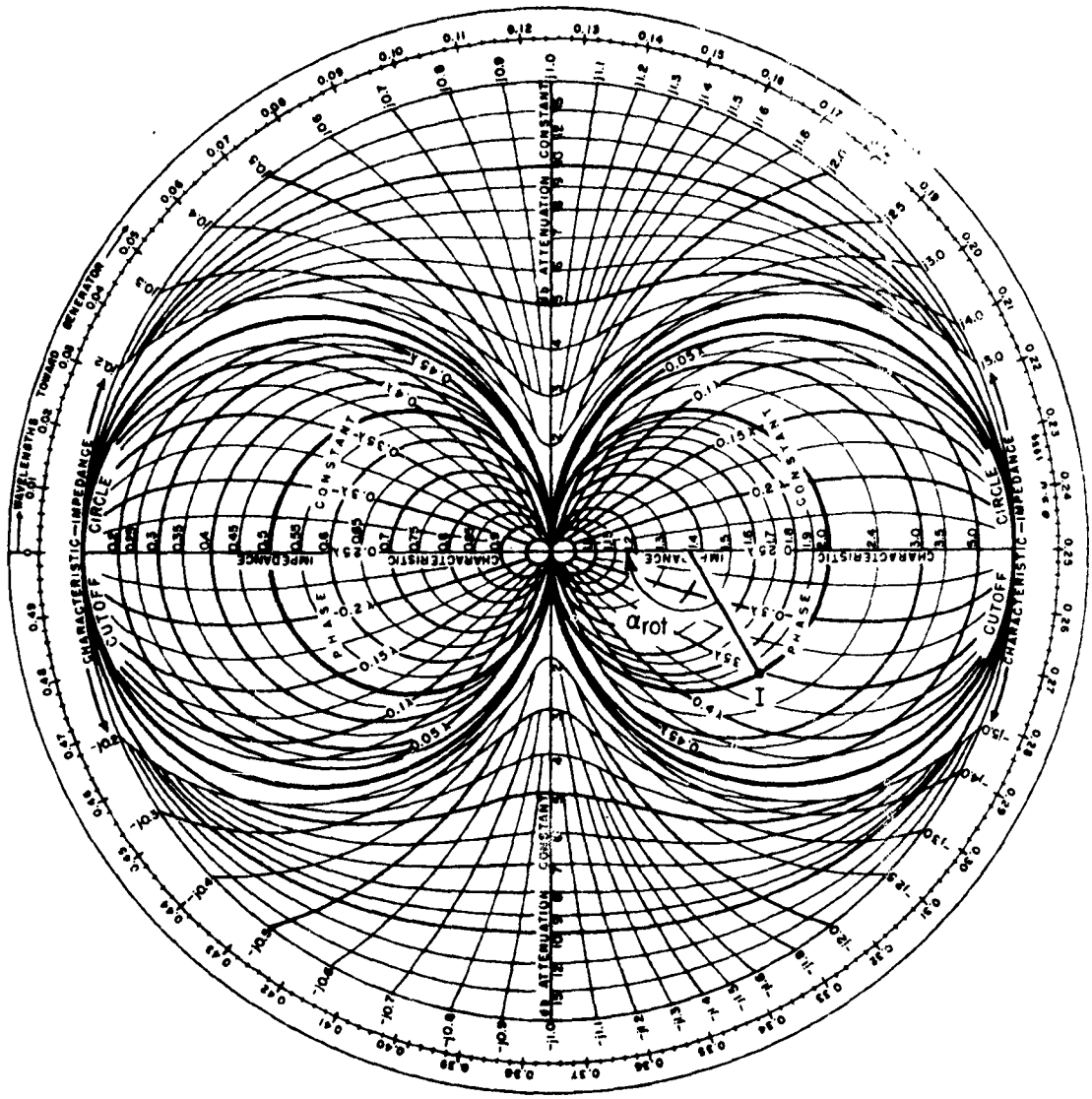

Fig. 14. A grid of constant impedance and constant phase shift (or attenuation) curves.

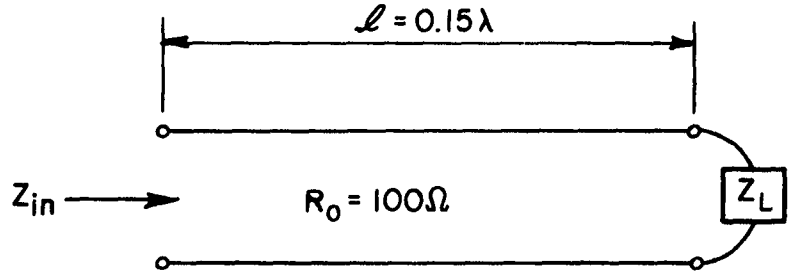

Fig. 15. A simple network used as an example.

the paper. It is in this light that the following constructions within this circle are developed. The point Z_L'/R_N is inverted through I to the point, A, by means of the construction in dotted lines; this point is inverted through 0 to B which is then rotated by angle α_{rot}, to Z_{in}/R_N. This orthographic projection of the normalized input impedance is transformed into the stereographic projection via the butterfly diagram to the point Z_{in}/R_N. Admittedly, this is an inconvenient construction which the author developed before the publication of a much simpler construction by Mathis,[11] but is does unify the presentation around the inversion-rotation operation within the Poincaré sphere.

The representation of a two-port network by an inversion-rotation operation is useful for certain applications. One of these is the design of a "phase amplifier", that is a device which when loaded with two impedances which differ in the phase of their reflection coefficients by $\Delta\phi$ cause a change of phase in input reflection coefficient, $A\Delta\phi$ where $0 \leq A \leq \infty$ is the phase gain. For very simple networks this does not present much of an advantage, but for complicated networks involving a variety of lengths and characteristic impedances and lumped elements, this technique proves efficient.

For example, if a load switches between $Z_{L1}/R_N = j0.5$ and $Z_{L2}/R_N = j0.1$, representing a phase change in load reflection coefficient $\Delta\phi = 42^o$ as shown in Fig. 18, and an amplification factor A = 2 was desired, the locus of all inversion points, I, yielding this amplification factor is given by the circle derived as shown in Fig. 18. Points P and Q are arbitrarily located points separated by $A\Delta\phi = 84^o$. By overlaying Fig. 3 on this diagram, it is clear that a transmission line of electrical length

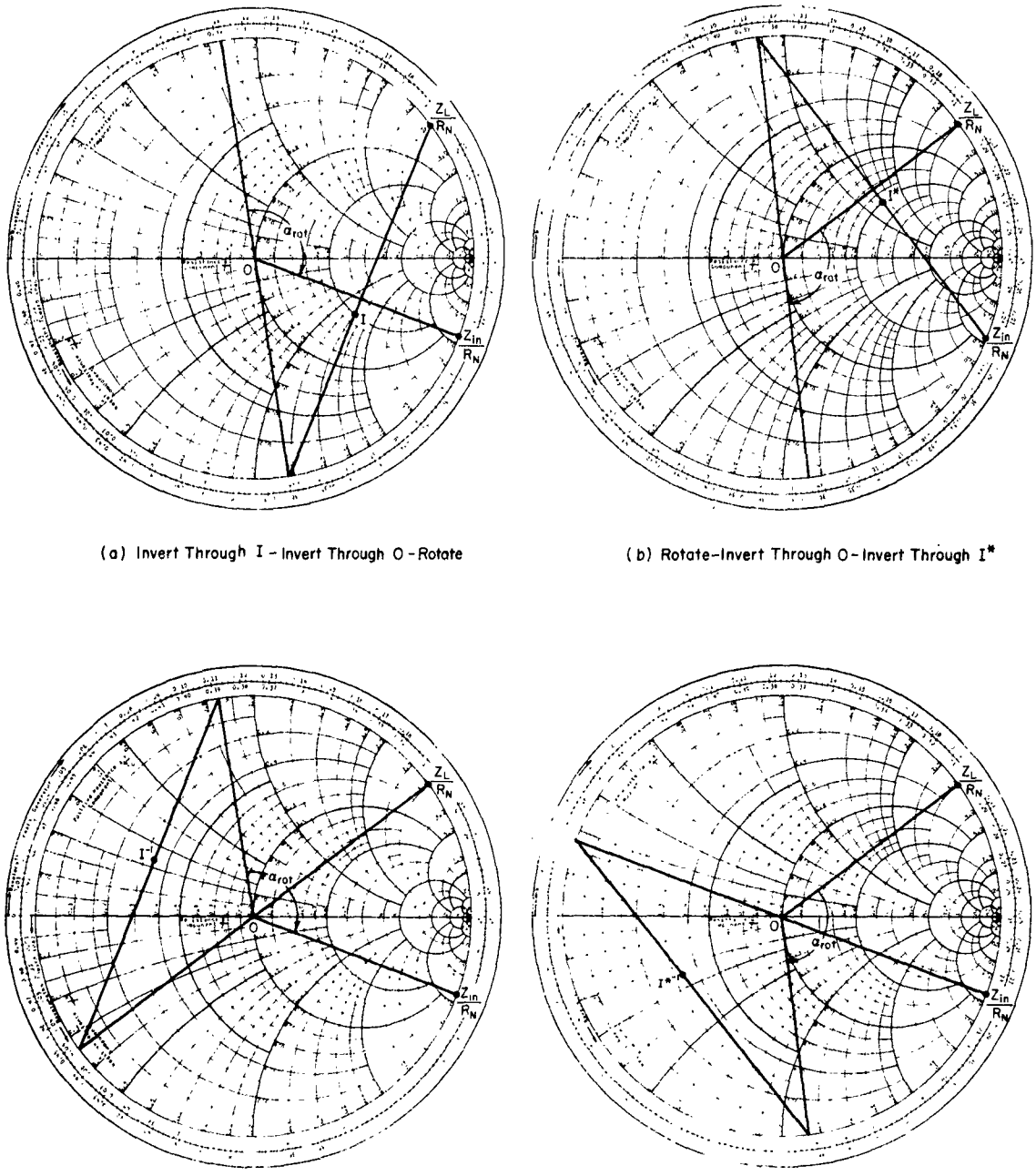

(a) Invert Through I - Invert Through O - Rotate

(b) Rotate-Invert Through O - Invert Through I^*

(c) Invert Through O - Invert Through I^{-1} - Rotate

(d) Rotate - Invert Through I^{*-1} - Invert Through O

Fig. 16. Inversion-rotation construction associated with the network of Fig. 15.

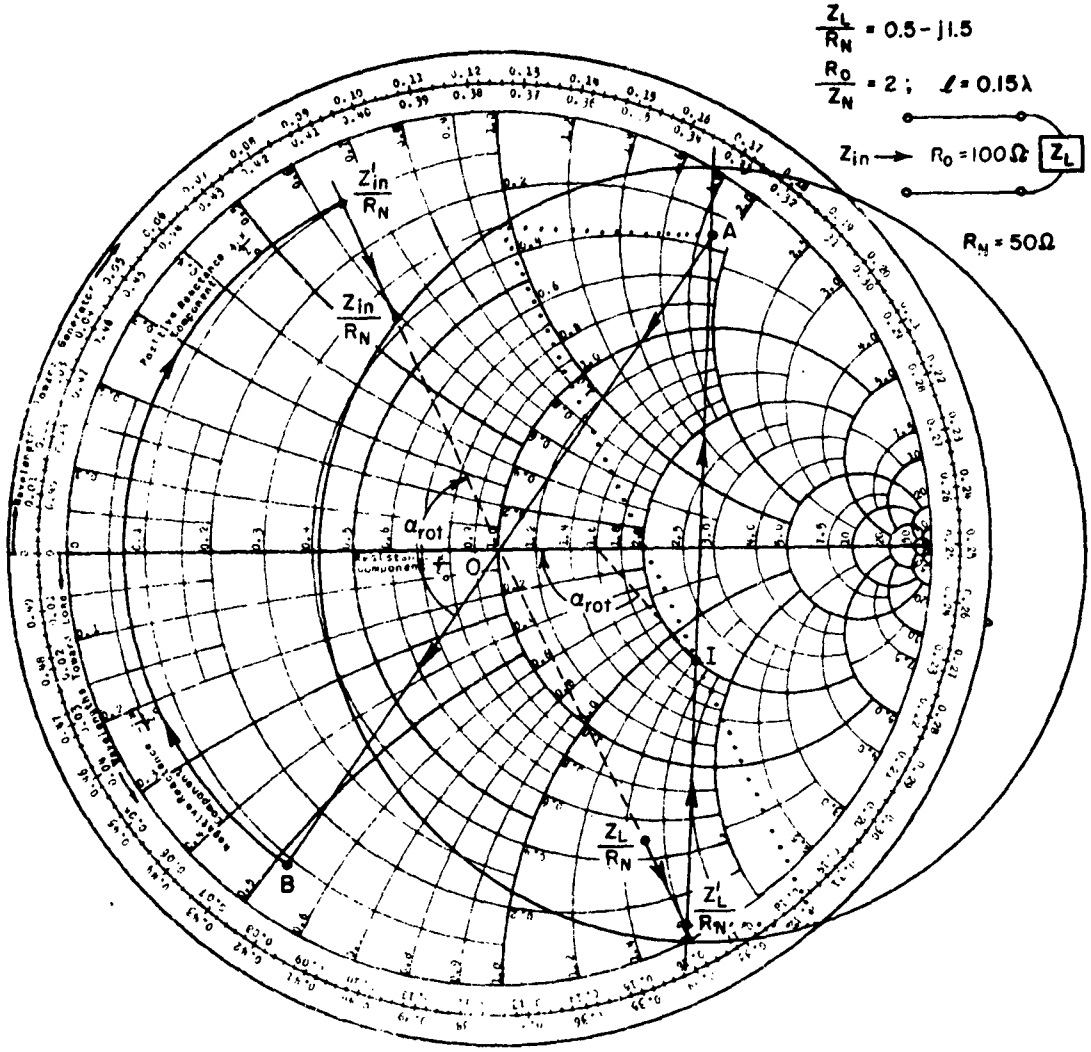

Fig. 17. An example of the inversion-rotation operation for a lossy load.

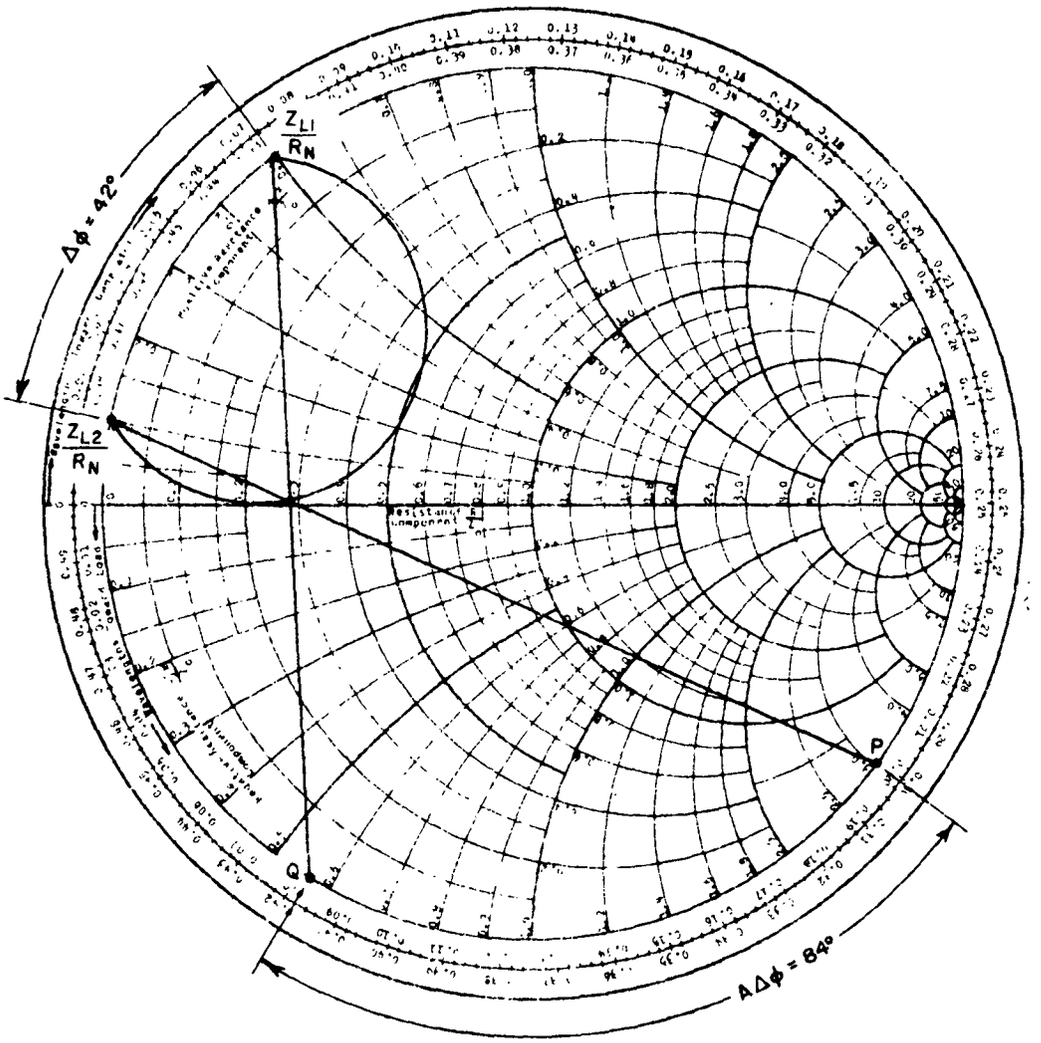

Fig. 18. An illustration of a "phase amplifier" with a gain of two.

$\beta\ell = 0.2\lambda$ and characteristic-impedance $Z_C = 0.65\ R_N$ would be one network which would achieve the desired amplification.

Alternatively, one may ask, given a lossless network, what two reactive loads separated by $\Delta\phi$ effect a maximum phase amplification? Since the inversion point, I, may be plotted for the network, clearly the desired loads are those which are rotated $\pm\Delta\phi/2$ from the line joining 0 and I, as sketched in Fig. 19.

Obviously, working with lossy loads detracts from the utility of the inversion method for design purposes.

Next, consider the problem of cascading two-port networks. Figures 20 a,b show symmetrical networks and their respective inversion centers. Figure 20 c shows a construction utilizing these inversion centers to obtain the inversion center of the composite network as well as its rotation angle. The construction may be explained as follows: to transform through the composite network shown in Fig. 20 c, recalling the alternatives given in Fig. 16, the sequence of operations is: from the reactive load, rotate 53° ccw (i.e., 307° cw), invert through $I_2^{*\,-1}$, invert through 0, invert through 0, invert through I_1^{-1}, rotate 85° cw, rotate Δ° cw to the input reactance. This last rotation is due to the asymmetrical nature of the network as will be discussed below. To find Δ, one load (e.g., a short circuit) is transformed through the network in the usual manner and the result is compared with that obtained by the method just outlined. In this case Δ is found to be 35° cw. Next, consider the two loads Z_{L1}/R_N and Z_{L2}/R_N separated by angle Ω and indicated in Fig. 20c; after the initial 53° ccw rotation discussed above Z_{L1}/R_N will appear at A and Z_{L2}/R_N will appear at B. By the nature of the rest of the geometrical constructions, we are assured that the input impedances corresponding to these two loads will also be separated by an angle Ω. The question then arises, if this same result is to be achieved by a simple inversion operation followed by a rotation, where must the inversion point lie? Clearly, one obvious choice would be the center of the chart, 0, since any two points separated by an angle Ω would transform through 0 to corresponding points also separated by Ω. Reasoning thus, a circle passing through A, 0, and B can be drawn, which, by well known geometrical properties of the circle, is the locus of the inversion center we seek. To establish its exact location on this circle, we reason as follows: loads Z_{L3}/R_N and Z_{L4}/R_N, indicated in Fig. 20 c, appear at points C and D respectively; upon inversion through $I_2^{*\,-1}$ and 0, points C and D remain unchanged and upon further inversion through I_1 and 0 they end up separated by an angle ω. As before, if a simple inversion-rotation operation is to achieve this same result, the inversion center must lie on a circle fixed by C, D, and I_1.

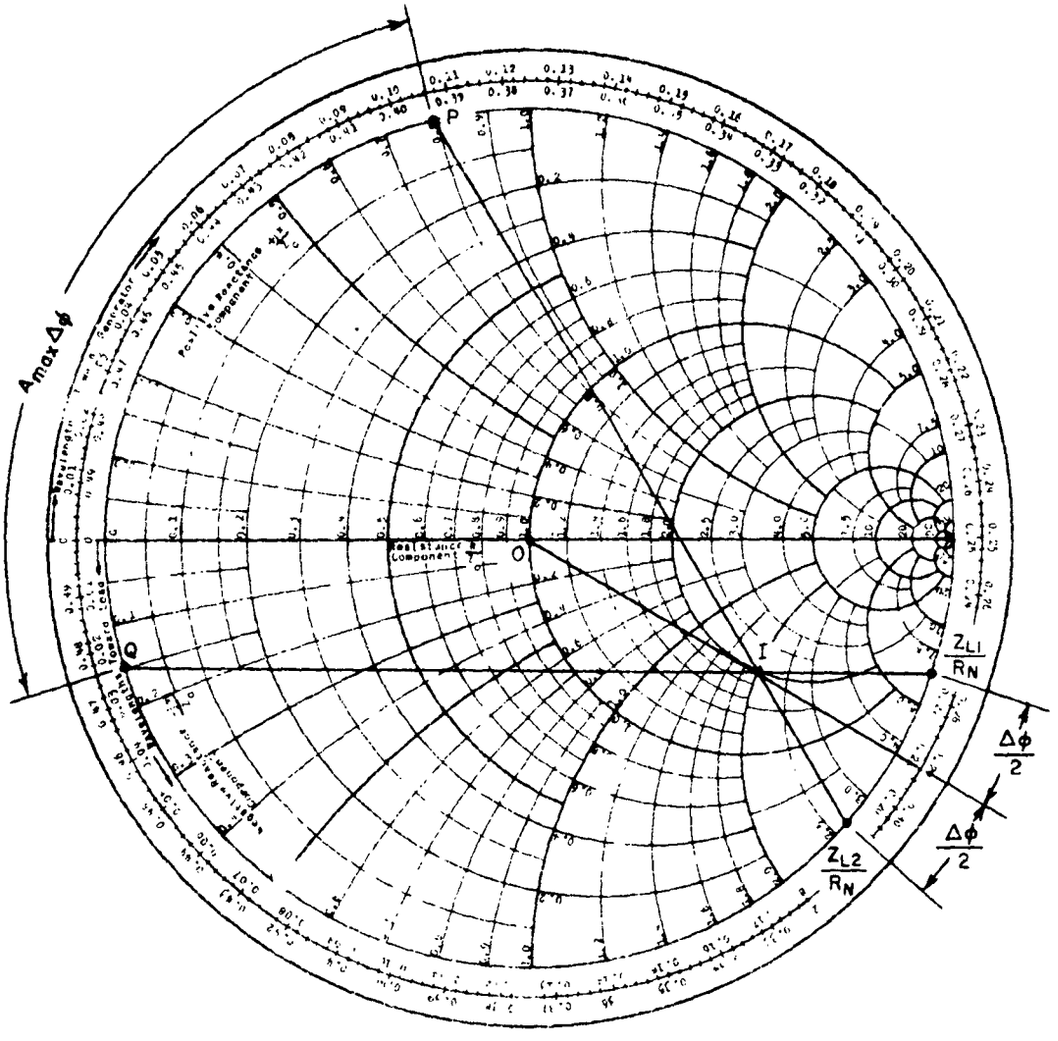

Fig. 19. The location of the inversion point for maximum phase amplification.

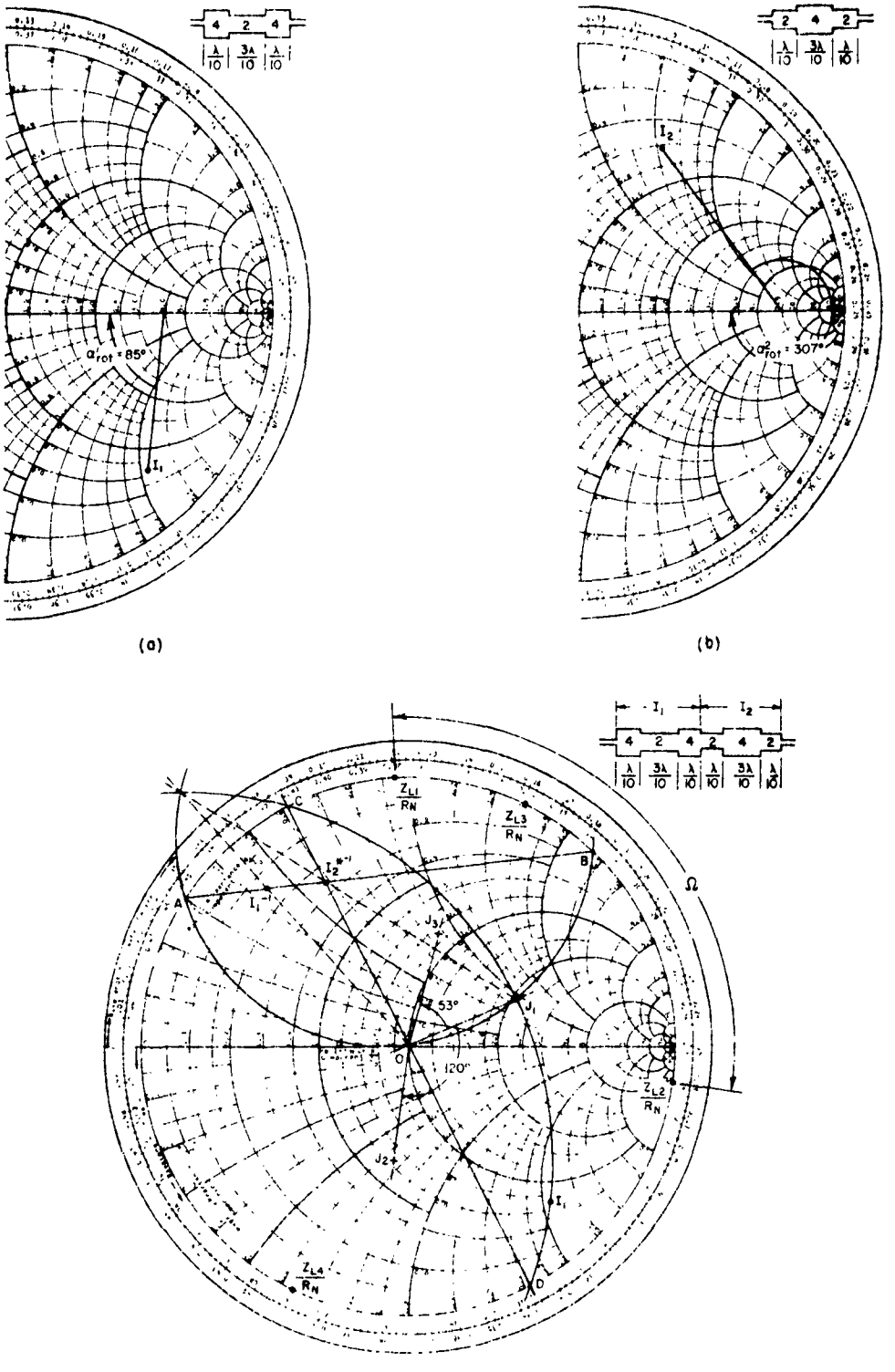

Fig. 20. The construction relating the location of the inversion points of two networks and that for the two networks in tandem.

To satisfy both the conditions discussed above, the inversion point must lie at the unique point, J_1, which is the intersection of the two circles. This point may also be obtained by the construction given in dashed lines in conjunction with the circle A-0-B.

Once J_1 is found, the transformation process is as follows: rotate 53° ccw, invert through J_1, invert through 0, rotate 120° cw (85° cw + 35° cw). Alternative constructions can be devised; for example, if J_2 is used, the process is, rotate 67° cw (53° ccw + 120° cw), invert through J_2, invert 0; or, if J_3 is used, the process is, invert through J_3, invert through 0, rotate 173° cw (120° cw - 53° ccw). Others may be found simply by transposing inversions and rotation and rotating the inversion point accordingly.

It is interesting to observe that the inverse process may be used to decompose the asymmetric network into symmetric networks in cascade.

The rotation-inversion concept holds for asymmetric networks as well as symmetric ones as was implied by the previous example. However, for asymmetric networks the rotation angle is not inflexibly fixed by the location of the inversion point and the concept of characteristic impedance loses its meaning. The inversion point I may be located as shown in Fig. 21 where $\overline{SC}$, $\overline{OC}$, $\overline{+j}$, $\overline{-j}$ represent the normalized input impedances corresponding to loads at SC, OC, +j, -j. The angle α_{rot} is found by applying the inversion operation through I and 0 to one of the loads and noting what rotation is required to end up at its corresponding input reactance.

The foregoing geometrical techniques were studied to provide simple working tools for the design of phase amplifiers and modulators utilizing transmission line elements. In particular, semiconductor diode loads were of interest because by rapidly modulating their bias with a square wave, an effective switching between two loads could be accomplished. Enhanced phase shift could then be achieved by interposing a two-port network between the diode and the remainder of the circuit, such as an antenna.

C. An Experimental Technique to Aid Decoupling Studies

A structure supporting many antennas, such as a ship, can be viewed as a lossy n-port network, each pair of antenna terminals forming a port which in general is coupled to all the other ports. To couple minimally these ports experimentally by varying the types, positions, etc. of the antennas is, to say the least, a tedious undertaking. If some scheme were devised whereby the relative power coupling between

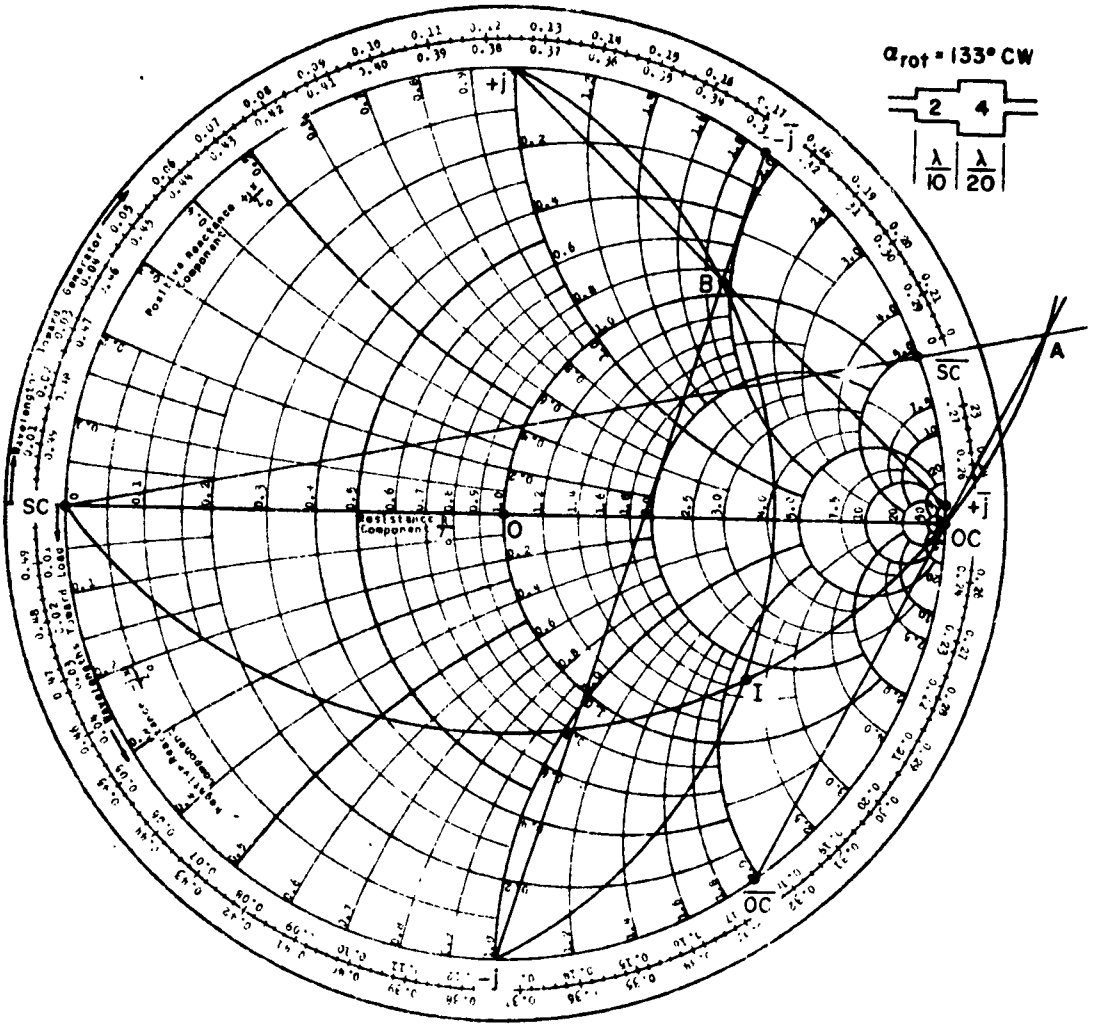

Fig. 21. The location of the inversion point and rotation angle for asymmetrical networks.

all ports could be detected simultaneously, a great advantage would be gained in experimental studies. This section discusses an attempt to devise such a scheme.

In essence, the idea is this: one port of the N + 1-port network is excited such that the incident and reflected waves can be separated (e.g., by an hybrid tee as in conventional cw scatter ranges) and each of the remaining N ports is terminated in loads which can be switched between two values at rapid rates. Previous work[12,13,14,15] has shown that such a load variation produces a modulation of the scattered wave which is related to the particular loads used and the input impedance at the loaded port. In practice, each port is loaded with a semiconductor diode, which upon square wave modulation of its bias, effects a rapid switching between two load values. The modulation frequencies at the loaded ports are related by powers of 2, e.g., f_1 = 400 cps, f_2 = 200 cps, f_3 = 100 cps, etc. for reasons which will become clear later.

Consider Fig. 22 which is a sketch of N+1 antennas arranged as described above and all coupled to one another. The #0 is the transmit-receive antenna and the remaining ones are diode loaded. Clearly, if the #n^{th} antenna load alone is modulated, the signal received by the #0 antenna will be square wave modulated at a frequency $f_1/2^{n-1}$ with its magnitude related to the coupling between the #n and the #0 antennas. If in addition a second antenna, say #2, is square wave modulated at a frequency $f_1/2^1$, the signal received by the #0 antenna will comprise a sum of three waves, i.e., one which proceeds from #0 to #2 and back modulated at $f_1/2^1$, one which proceeds from #0 to #n and back modulated at $f_1/2^{n-1}$ and one which proceeds from #0 to #2 to #n and back to #0 (and vice versa). This latter wave is related to the coupling between #0 and #n and will have a modulation waveform which is the product of the square waveforms impressed on #2 and #n. We shall now consider such waveforms in detail.

Figure 23a shows three typical unit square waveforms used to modulate three diodes; they are designated by $e_{01}(t)$, $e_{02}(t)$, and $e_{04}(t)$ in which the subscripts indicate the relationship between the period of each wave to the period of the highest frequency wave. It is noted that each of these waveforms is an odd function with respect to the t = 0 abscissa. Figure 23b shows the three even waveforms obtained by taking the various products of the three waveforms of Fig. 23a; the notation is unambiguously defined in the sketch. It may be verified that in the general case the following orthogonality relations hold among these functions:

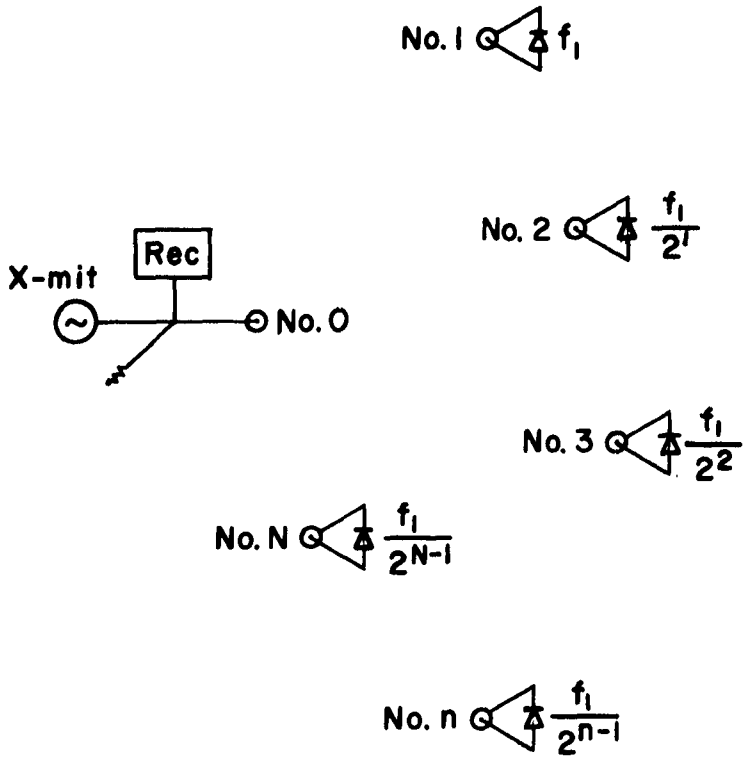

Fig. 22. A sketch of an N+1 port network formed by N+1 antennas. The 0^{th} antenna serves as a transmitter receiver and the remaining antennas are loaded with diodes.

$$(8) \qquad \frac{1}{T_m}\int_0^{T_m} e_{om}(t)\, e_{on}(t)\, dt = \begin{cases} 0 & m > n \\ 1 & m = n \end{cases} \qquad m,n = 1,2,4,8,\cdots$$

$$(9) \qquad \frac{1}{T_k}\int_0^{T_k} e_{mn}(t)\, e_{jk}(t)\, dt = \frac{1}{T_k}\int_0^{T_k} [e_{om}(t)e_{on}(t)]\cdot[e_{oj}(t)e_{ok}(t)]\, dt$$

$$= \left\{\begin{array}{ll} 0 \quad k > m,n,j & m,n \\ 1 \quad m=n=j=k & j,k \end{array}\right\} = 1,2,4,8,\cdots$$

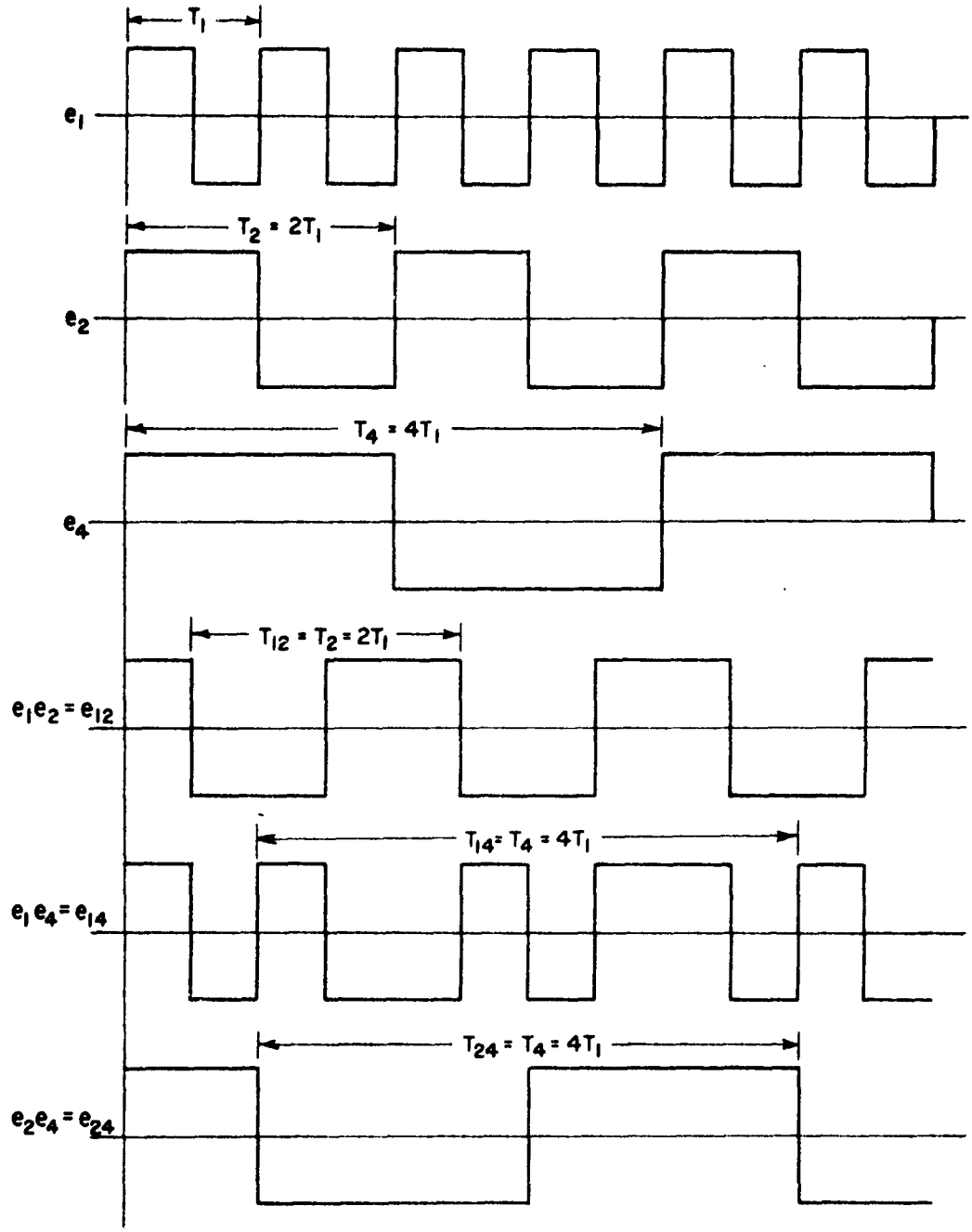

Fig. 23. Diode modulation waveforms and product waveforms.

$$(10) \qquad \frac{1}{T_k}\int_o^{T_k} e_{on}(t)e_{jk}(t)dt = \frac{1}{T_k}\int_o^{T_k} e_{on}(t)[e_{oj}(t)e_{ok}(t)]dt$$

$$= 0 \quad k \geq n, j \quad n,j,k=1,2,4,8,\cdots \ .$$

Hence, all waveforms are othrogonal to one another. And since each individual waveform can be expressed as a Fourier series which is complete over the interval 0 to T_k, the square waves also form a complete set and may be used to synthesize any composite waveform. That is, if the composite waveform at the receiver has a form e(t), it may be expanded as

$$(11) \qquad e(t) = \frac{1}{2}\sum_{p=0}^{N}\sum_{q=0}^{N} a_{pq}\, e_{pq}(t), \qquad e_{oo} \equiv 1 \qquad e_{mn} = e_{nm}$$

where the weighting coefficients, a_{pq}, are obtained using the orthogonality relations

$$(12) \qquad a_{pq} = \frac{2}{T_p}\int_o^{T_p} e(t)\, e_{pq}(t)\, dt \qquad p \geq q.$$

In general, the composite function e(t) and the coefficients a_{pq} are complex quantities; for this reason, the detection system behind the #0 antenna must be phase sensitive to obtain quadrature components of the scattered signal.[16]

Unfortunately the weighting coefficients, a_{pq}, are not directly proportional to the coupling between the p^{th} and q^{th} antennas. Their amplitudes must be multiplied by factors obtained in the rather complicated fashion shown in Fig. 24. Points Z_{L1}/R_N and Z_{L2}/R_N are plotted on a Smith Chart at the two loads between which switching is effected at the n^{th} port and I^* is located at Z^*_{nn}/R_N where Z^*_{nn} is the complex conjugate of the input impedance at that port; then the coefficient a_{on} is multiplied by a factor, m_{on}, found from the circle on which I^* lies in Fig. 13. In terms of the phase gain, A, (Fig. 18) $m_{on} = \tan\alpha/\tan A\alpha$. Likewise, $m_{mn} = m_{om}\, m_{on}$.

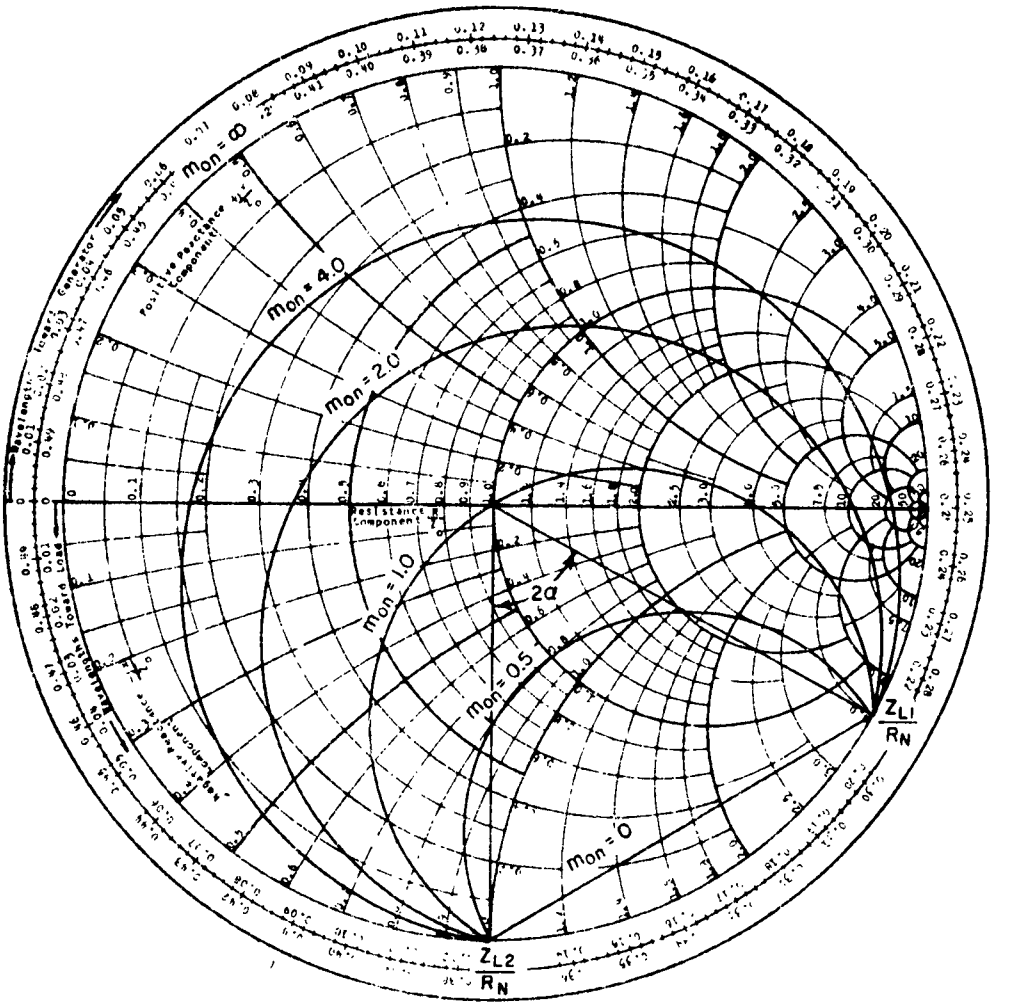

Fig. 24. A diagram for finding the factors, m_{on}.

The introduction of the factors, m, is the weakness of the technique. Clearly Z_{nn} is not a constant independent of the loads on all the terminals – the supposition that coupling exists means that Z_{nn} is dependent on the loads in general. If such dependence exists, then we say that the antennas are impedance decoupled and in terms of the technique just described, all the product coefficients, $a_{mn}(m, n \neq 0)$, are zero. At the writing of this report we could see no way around this problem.